SUPPORTING INFORMATION

The synthesis and supramolecular organization of chiral and achiral conjugated star-polymers

*Marie-Paule Van Den Eede[1], Julien De Winter[3], Pascal Gerbaux[3], Joan Teyssandier[2], Steven De Feyter[2], Cédric Van Goethem[4], F. J. Ivo Vankelecom[4] and Guy Koeckelberghs[1]**

[1]Laboratory for Polymer Synthesis, Department of Chemistry, KU Leuven, Celestijnenlaan 200F, B-3001 Heverlee, BELGIUM

[2]Division of Molecular Imaging and Photonics, Department of Chemistry, KU Leuven, Celestijnenlaan 200F, B-3001 Heverlee, BELGIUM

[3]Organic Synthesis and Mass Spectrometry Laboratory, Interdisciplinary Center for Mass Spectrometry, University of Mons-UMONS, 23 Place du Parc, 7000 Mons, BELGIUM

[4]Center for Surface Chemistry and Catalysis, Department of Microbial and Molecular Systems, KU Leuven, Celestijnenlaan 200F, B-3001 Heverlee, BELGIUM

TABLE OF CONTENTS

EXPERIMENTAL INFORMATION

All reagents were purchased from Sigma Aldrich, TCI, Acros organics, and J&K scientific. Gel permeation chromatography (GPC) measurements were carried out with a Shimadzu LC20 apparatus (LC-20AT pump, CBM-20A controller, RID-20A and SPD-20A detectors, PLgel 5 μm MIXED-D column). The measurements were performed in tetrahydrofurane (THF) as eluent toward poly(styrene) standards. ^{1}H NMR measurements were done with a Bruker Avance 300 MHz for the monomers and polymers, and a Bruker Avance 400 MHz for the initiators. UV-vis and CD spectra were obtained respectively with a Perkin Elmer Lambda 900 and a JASCO J-810 spectrometer. Fluorescence spectra were recorded on an Edinburgh Instruments LLS980 Steady-State spectro-fluorimeter. Excitation was done with a 450W xenon lamp and the emission was measured with an extended red-sensitive photomultiplier. All fluorescence spectra were absorption corrected by dividing the obtained emission values by the absorption values obtained at the wavelength of excitation. The samples were measured in quartz cuvettes with an optical pathway of 1 cm. The melting and crystallization behavior of the polymer was investigated using DSC. The measurements were performed with a TA Instruments Q2000-DSC. DSC samples were put in Tzero Aluminium Hermetic pans and calibration was done towards indium. A heating rate of 10 °C/min was used. AFM was performed on dry films obtained by drop-casting on a freshly cleaved highly oriented pyrolytic graphite sample (HOPG, grade ZYB, Advanced Ceramics Inc., Cleveland, USA) 0.1 mg/ml solutions of the polymers in various solvents (chloroform, toluene and chloroform/methanol (1:1) mixture). Deposition occurred in saturated atmosphere to allow solvent to evaporate overnight in order to let the system approach thermodynamic conditions. In the case of the chloroform/methanol mixtures, a 0.2 mg/ml solution of the polymer in chloroform was first deposited on the surface, and an equivalent volume of pure methanol was added immediately after. AFM measurements were carried out in air using a Multimode AFM with a Nanoscope

VIII controller (Veeco/Digital Instruments) in intermittent contact mode. Olympus silicon cantilevers (OMCL-AC160TS) were used. AFM images were processed using WSxM (Nanotec Electronica, Spain) software.[3] Matrix-assisted laser desorption/ionization time-of-flight (MALDI-ToF) mass spectra were recorded using a Waters QToF Premier mass spectrometer equipped with a Nd-YAG laser of 355 nm with a maximum pulse energy of 65μJ delivered to the sample at 50 Hz repeating rate. Time-of-flight mass analyses were performed in the reflection mode at a resolution of about 10 000. The matrix, trans-2-(3-(4-tert-butyl-phenyl)-2-methyl-2-propenylidene)malononitrile (DCTB), was prepared as a 40 mg/mL solution in chloroform. The matrix solution (1 μL) was applied to a stainless steel target and air-dried. Polymer samples were dissolved in chloroform to obtain 1 mg/mL solutions. Then, 1 μL aliquots of these solutions were applied onto the target area (already bearing the matrix crystals) and then air-dried. TEM images were acquired after drop-casting a 0.1 mg/mL solution on a Holey carbon coated TEM grid (Cu, 300 mesh, Pacific Grid Tech). Images were acquired using a probe-abberation corrected JEOL ARM-200F operated at 200 kV.

SYNTHESIS OF THE PRECURSOR MONOMERS

2-bromo-5-iodo-3-octylthiophene **3** and (+)-(*S*)-2-bromo-5-iodo-3-(3,7-dimethyloctyl)thiophene **4*** were synthesized according to literature procedures.[1]

SYNTHESIS OF THE PRECURSOR INITIATOR

Precursor initiator bromo-[2-methyl-2-[(tert-butyldimethylsilyloxy)-methyl]phenyl]bis(triphenylphosphine)nickel(II) **1** was prepared according to literature procedure[2], using $Ni(PPh_3)_4$ (4.43 g, 4.00 mmol) and 1-bromo-2-methyl-4-[[[(t-butyl)dimethylsilyl]oxy]methyl]benzene (1.89 g, 6.00 mmol).

Yield **1**: 0.236 g (6,6%)

SYNTHESIS OF THE POLYMERS

An overview of the polymerization of polymers **P1a** and **P1s** can be found in scheme S1.

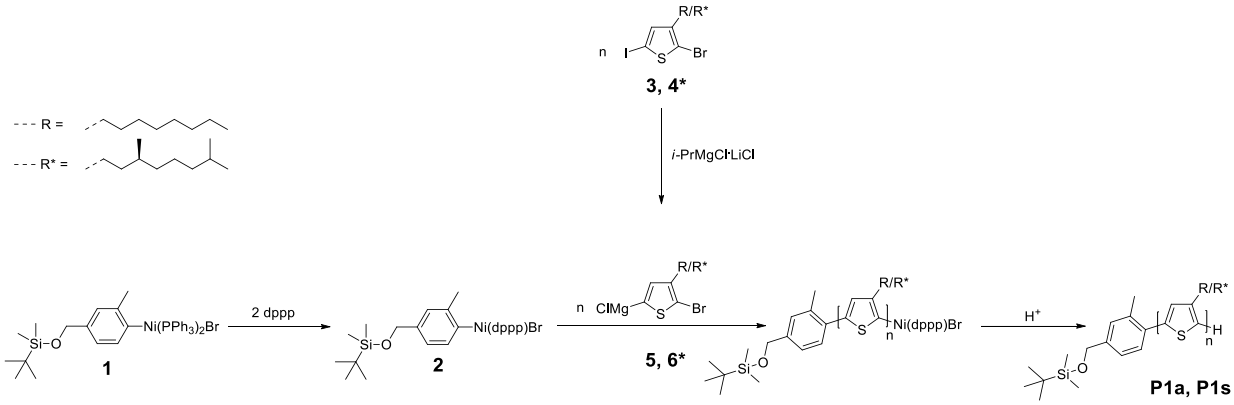

Scheme S1. Schematic representation of KCTP of polymers **P1a** and **P1s** with initiator **2**.

Precursor monomer 2-bromo-5-iodo-3-octylthiophene (**3**) (0.925 mmol; 0.371 g) was purged with nitrogen and dissolved in dry, degassed THF (8.55 ml). Next, *i*-PrMgCl·LiCl (0.925 mmol; 0.700 mL) was added and the solution was stirred for 40 minutes at 0°C. In the meantime a solution of precursor initiator **1** (0.0948 mmol; 85.2 mg) and dppp (0.190 mmol; 78.2 mg) in dry THF (3.00 mL) were purged with nitrogen, and stirred for 15 minutes. From the obtained

monomer solution 9.00 mL was transferred to the initiator mixture and stirred at room temperature for 50 minutes. The remaining 0.250 mL monomer solution was quenched with 0.50 mL of D_2O and analyzed by ^1H NMR. The polymerization was terminated with a 1M HCl in THF solution. The polymer solution was precipitated in methanol, filtered and fractionated by Soxhlet extraction with methanol and chloroform as solvents. Next, the chloroform fraction was concentrated, the polymer was precipitated in methanol, filtered, and dried under reduced pressure. Polymer **P1a** was obtained as a dark purple solid.

The same procedure was followed in order to obtain polymer **P1s**, by using precursor monomer **4**.

Yield: **P1a**: 0.169 g; **P1s**: 0.191 g

POSTPOLYMERIZATION DEPROTECTION

A schematic representation of the deprotection of polymers **P1a** and **P1s** in order to form **P2a** and **P2s**, can be found in scheme S2.

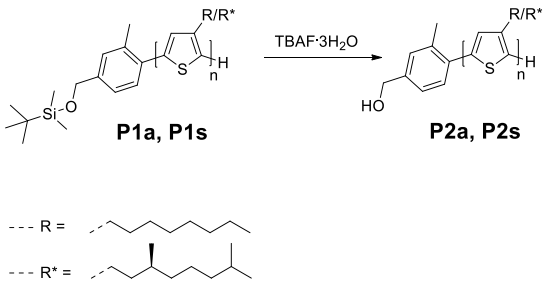

Scheme S2. Schematic representation of the deprotection of polymers **P1a** and **P1s**.

Polymer **P1a** (0.0424 mmol; 159 mg) was dissolved in 20.0 mL THF, purged with nitrogen and shielded from light. Next, $TBAF{\cdot}3H_2O$ (0.0678 mmol; 21.4 mg) was added and the mixture was stirred for 12 hours at room temperature. After reaction, the mixture was quenched with 20.0 mL H_2O and the polymer was extracted with chloroform. The polymer solution in

chloroform was dried over Na_2SO_4, filtered and concentrated under reduced pressure. Finally, the polymer was precipitated in methanol, filtered and dried in vacuo. Polymer **P2a** was recovered as a dark purple solid.

The same procedure was followed using polymer **P1s** in order to obtain **P2s**.

Yield: **P2a**: 0.153 g (99%); **P2s**: 0.162 g (95%)

POSTPOLYMERIZATION AZIDE FORMATION

A schematic representation of the azide formation on polymers **P2a** and **P2s** in order to form **P3a** and **P3s**, can be found in scheme S3.

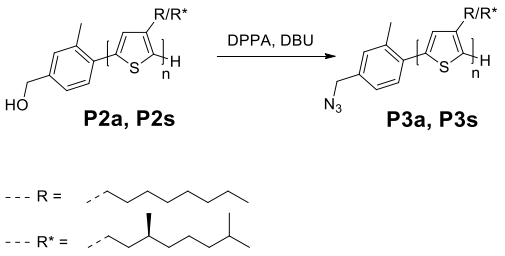

Scheme S3. Schematic represenation of the azide formation on polymers **P2a** and **P2s**.

Polymer **P2a** (0.0423 mmol; 0.153g) and DPPA (0.845 mmol; 0.233 g) were dissolved together in dry THF (20.0 mL), shielded from light and cooled to 0°C. Next, DBU (0.845 mmol; 0.129 g) was added stepwise. The polymer solution was stirred for 12 hours at room temperature. After reaction, the polymer was precipitated in methanol and filtered. The precipitate was washed with 50.0 mL of methanol and dried in vacuo. **P3a** was recovered as a dark purple solid.

Starting from polymer **P2s** (0.162 g), the same procedure was followed in order to obtain polymer **P3s**.

Yield: **P3a**: 0.144 g (93%); **P3s**: 0.152 g (93%)

POSTPOLYMERIZATION CLICK REACTION

A schematic representation of the click reaction of polymers **P3a** and **P3s** in order to form **P4a** and **P4s**, can be found in scheme S4.

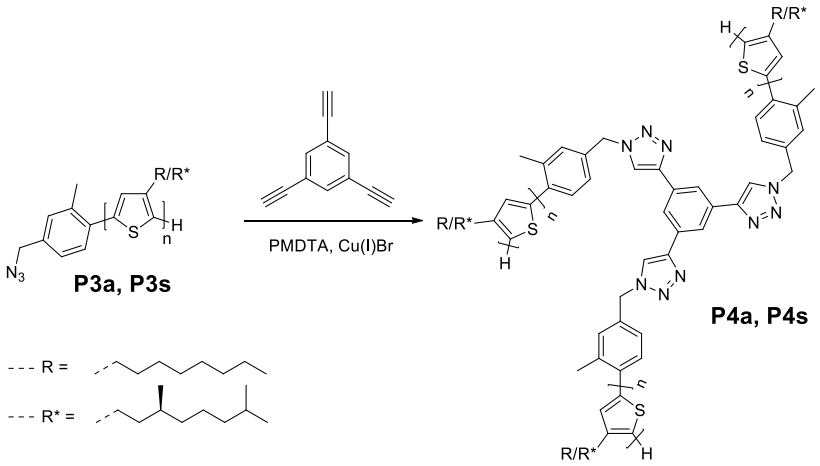

Scheme S4. Schematic representation of the click reaction of polymer **P3a** and **P3s**.

In a flask, polymer **P3a** (0.0395 mmol; 0.144g) and Cu(I)Br (0.00790 mmol; 1.13 mg) were dissolved in 10.0 mL dry THF, purged with nitrogen, and shielded from light. Next, a nitrogen purged solution of *N,N,N',N'',N''*-pentamethyldiethylenetriamine (PMDTA) (0.00790 mmol; 1.37 mg) in 0.500 mL dry THF was added to the polymer solution. To this mixture a nitrogen purged solution of 1,3,5-triethynylbenzene (0.0122 mmol; 1.84 mg) in 1.00 mL dry THF was added, and the mixture was stirred for 24 hours at room temperature. After complete reaction, an aqueous solution of NH_3 was added and the polymer was extracted with chloroform. The polymer solution was dried over Na_2SO_4, concentrated, precipitated in methanol, filtered and fractionated by Soxhlet extraction with methanol, acetone and chloroform as solvents. The polymer in the chloroform fraction was further purified with preparative GPC, precipitated in methanol, filtered and dried in order to obtain polymer **P4a** as a dark purple solid.

Starting from polymer **P3s** (0.152 g), the same procedure was followed in order to obtain polymer **P4s**.

Yield: **P4a**: 10.81 mg; **P4s**: 35.42 mg

^{1}H NMR SPECTRA OF THE POLYMERS

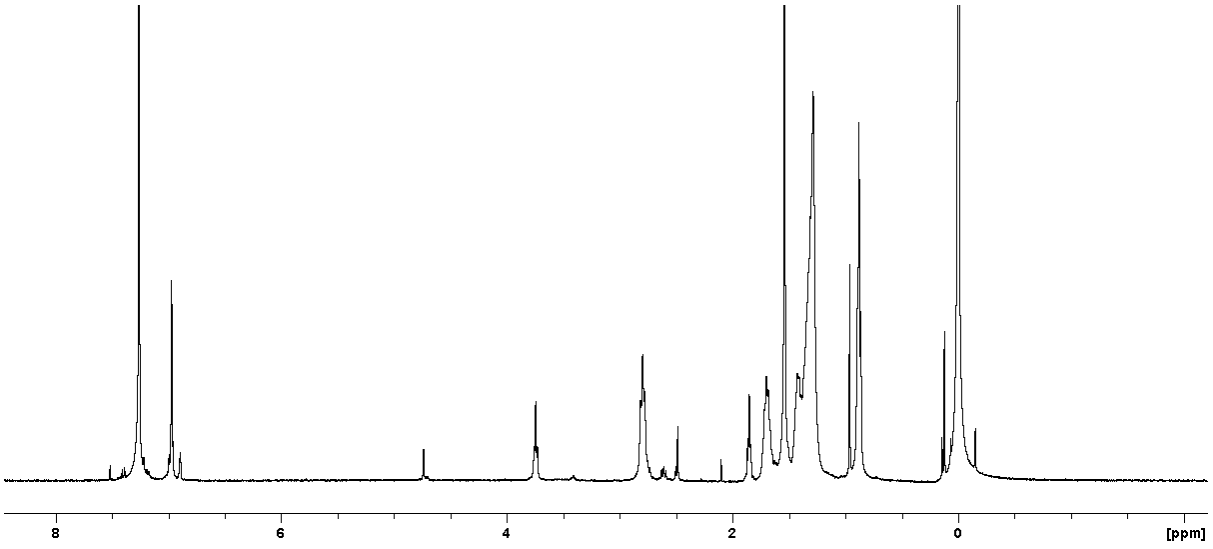

Figure 1S. ^{1}H NMR spectrum of **P1a** in $CDCl_3$.

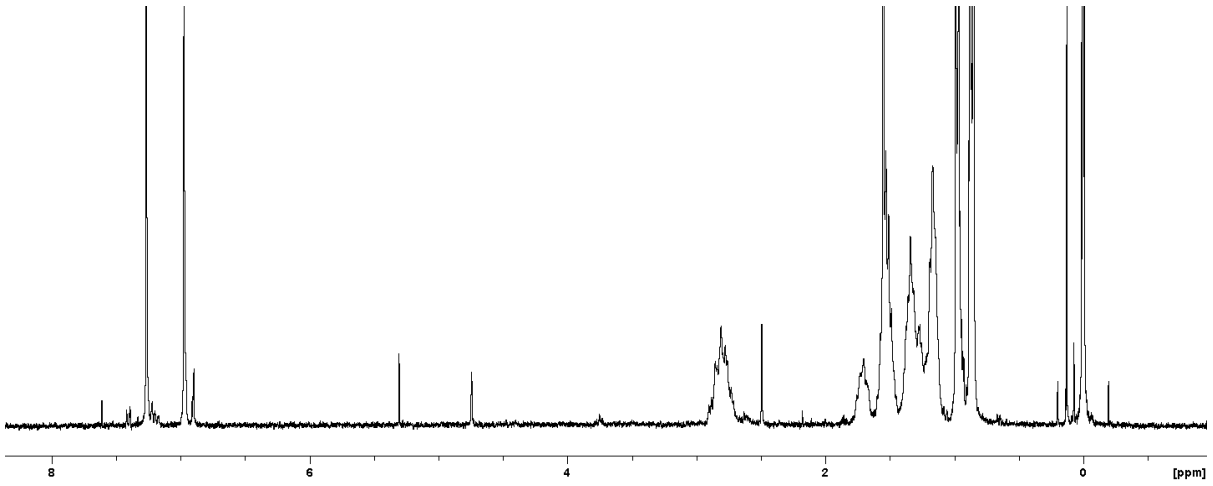

Figure S2. ^{1}H NMR spectrum of **P1s** in $CDCl_3$.

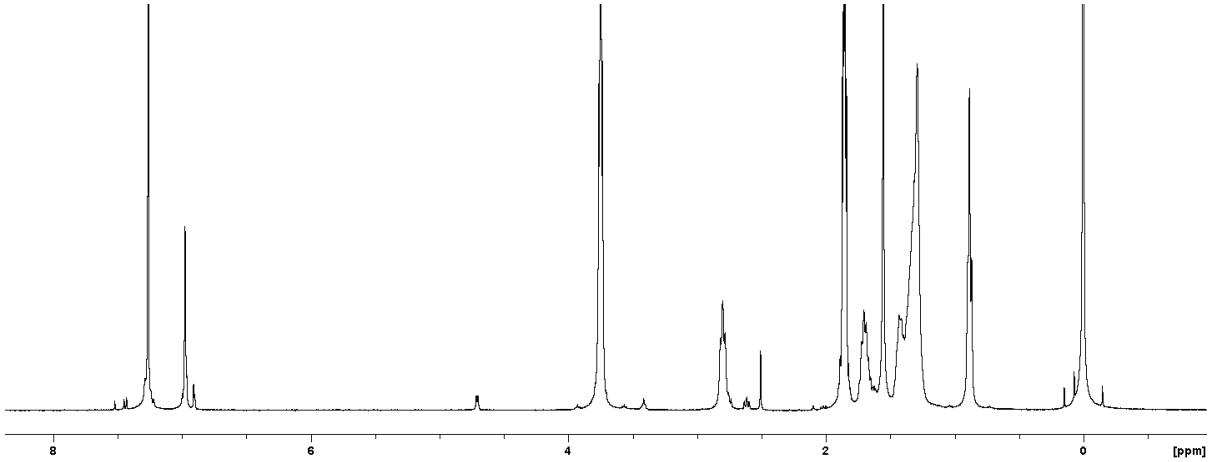

Figure S3. ^{1}H NMR spectrum of **P2a** in $CDCl_3$.

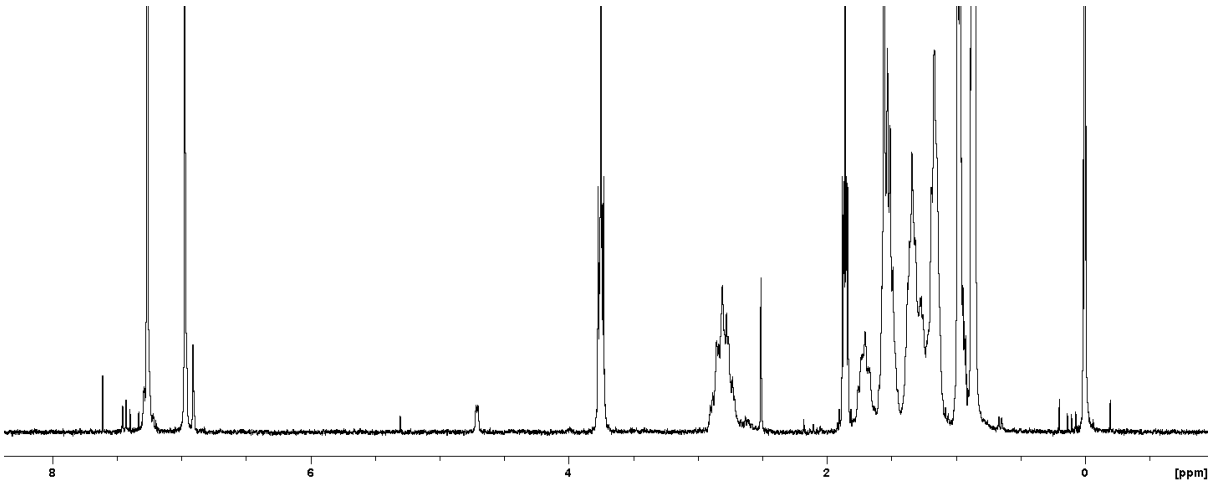

Figure S4. ^{1}H NMR spectrum of **P2s** in $CDCl_3$.

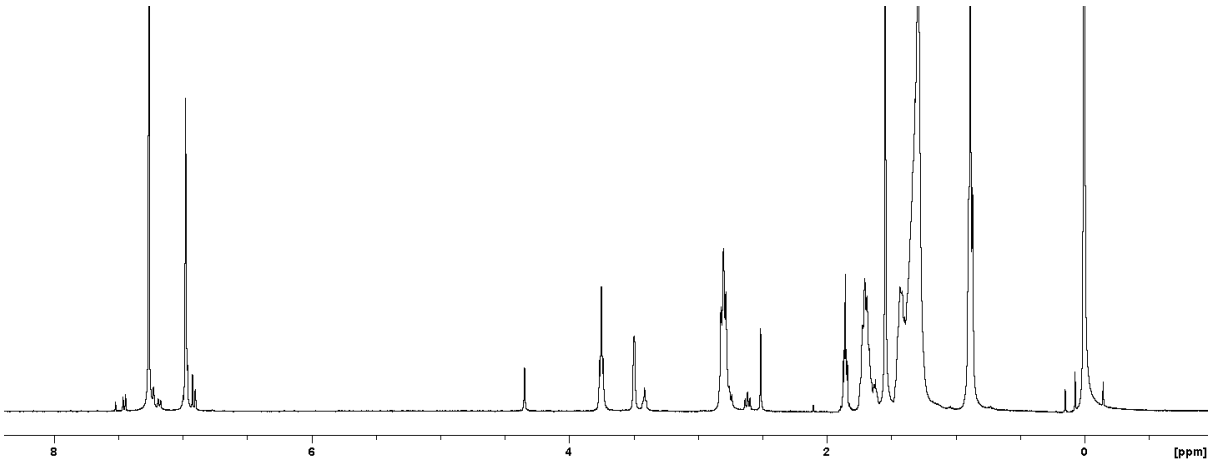

Figure S5. ^{1}H NMR spectrum of **P3a** in $CDCl_3$.

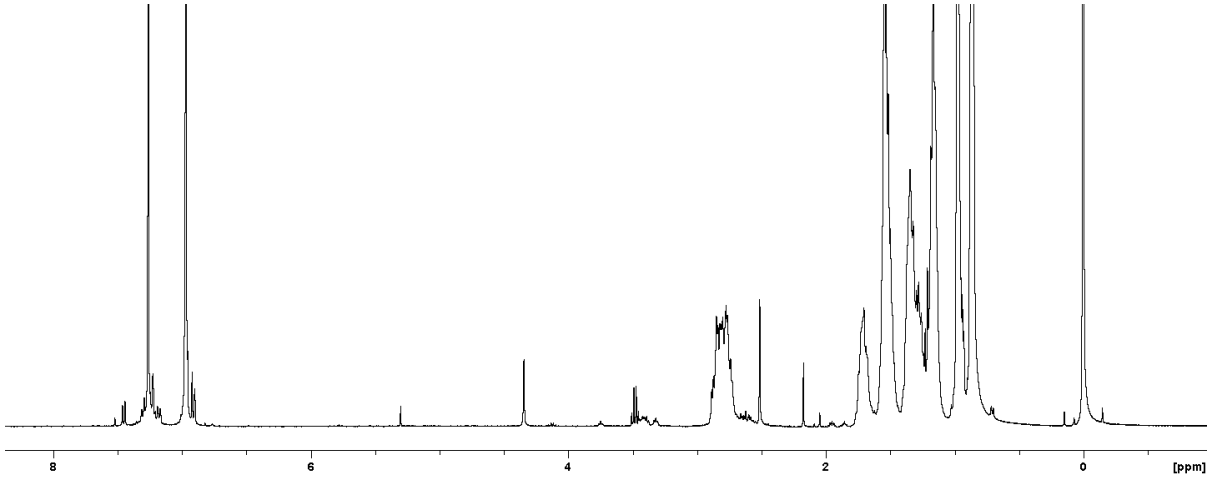

Figure S6. ^{1}H NMR spectrum of **P3s** in $CDCl_3$.

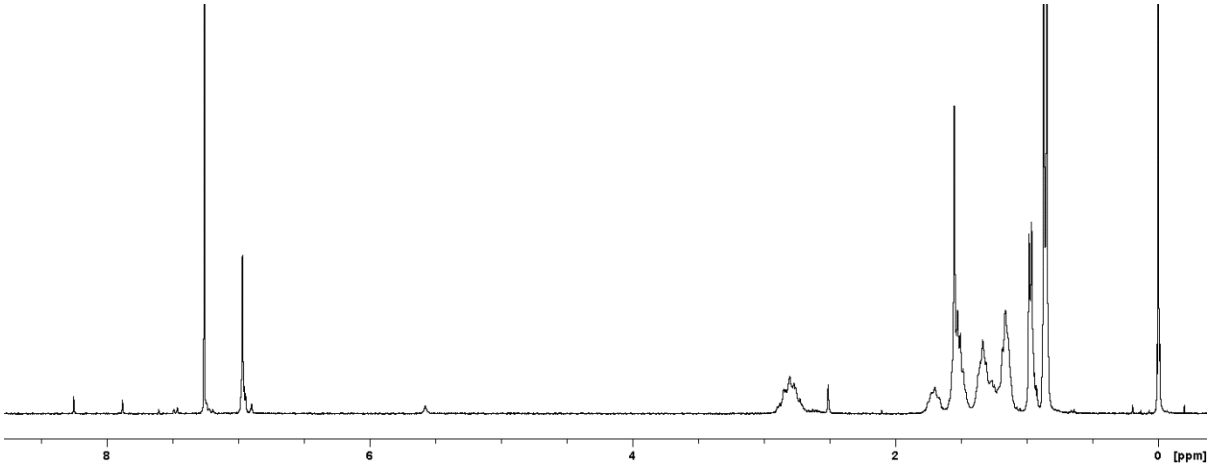

Figure S7. ^{1}H NMR spectrum of **P4a** in $CDCl_3$.

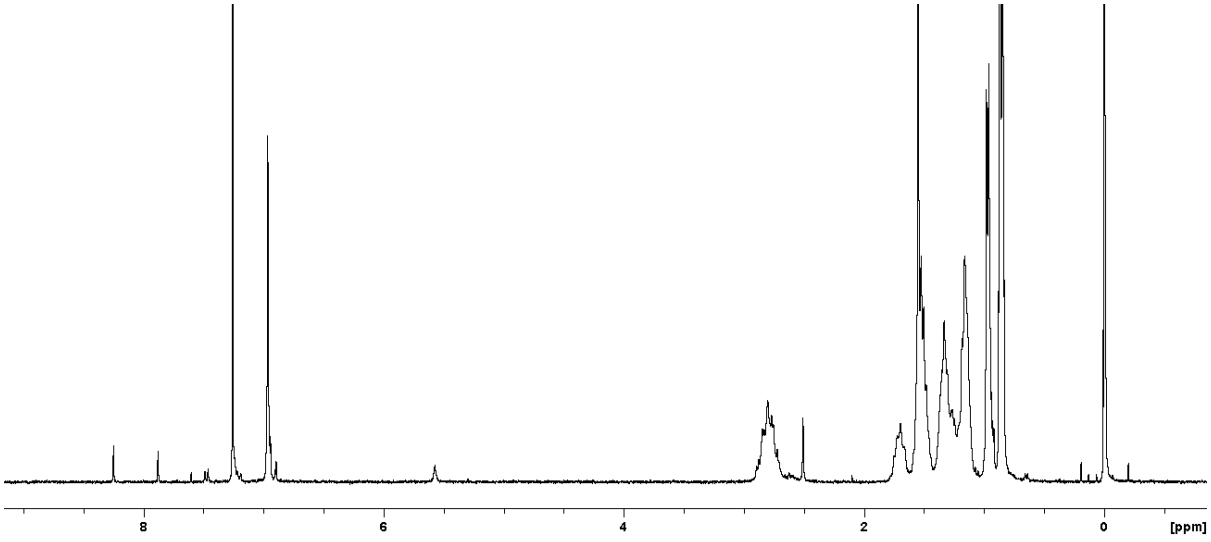

Figure S8. ^{1}H NMR spectrum of **P4s** in $CDCl_3$.

MALDI-ToF SPECTRA OF THE POLYMERS

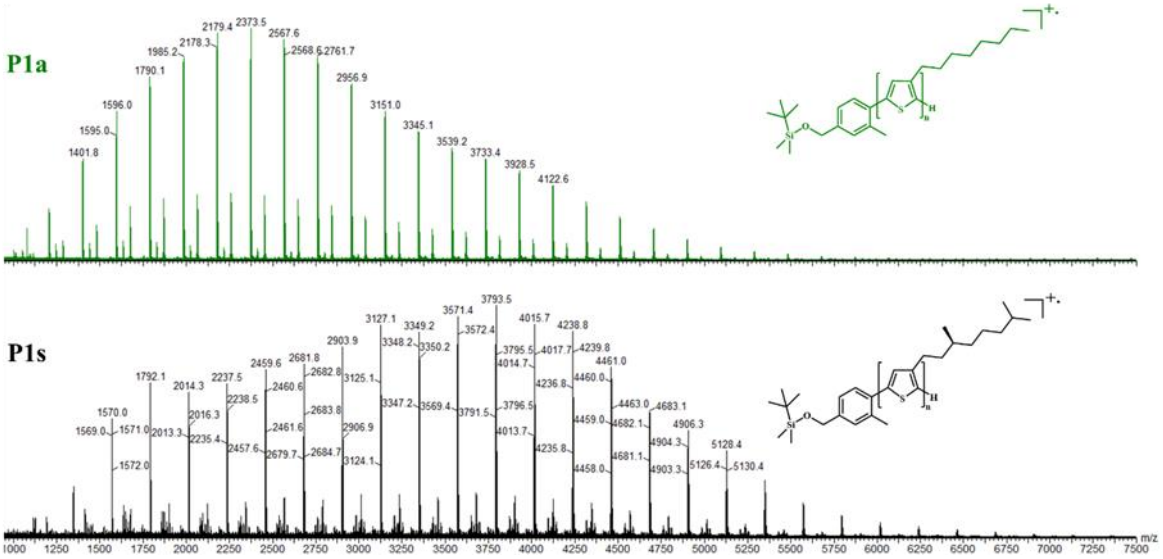

Figure S9. MALDI-ToF spectra of **P1a** and **P1s** before end-groups modification.

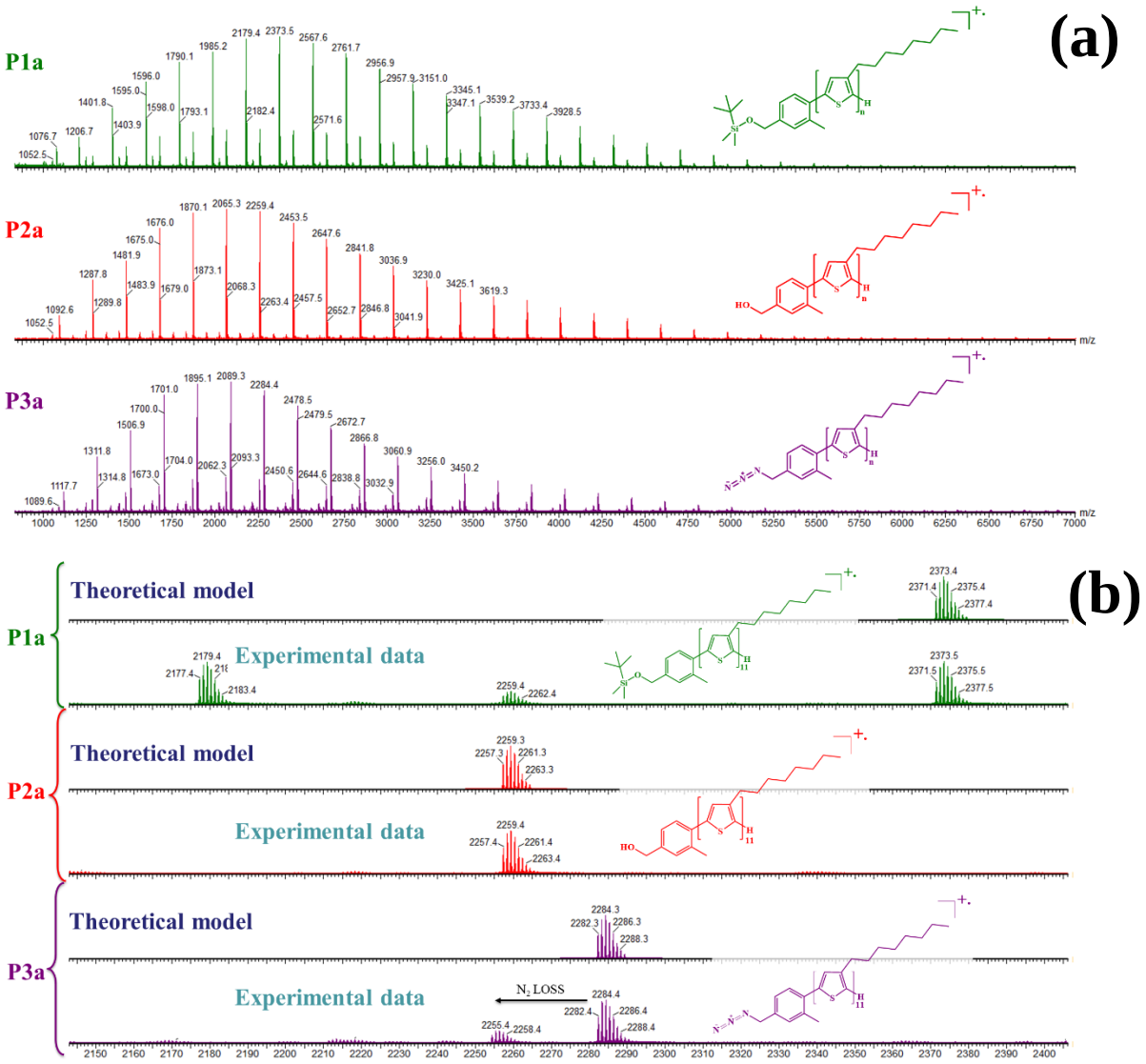

Figure S10. (a) global MALDI-ToF mass spectra for **P1a**-**P3a** and (b) magnification between *m/z* 2100 and m/z 2400 and comparison with isotopic model for 11-mers. Those mass spectra highlights the end-groups modification and proves the absence of degradation.

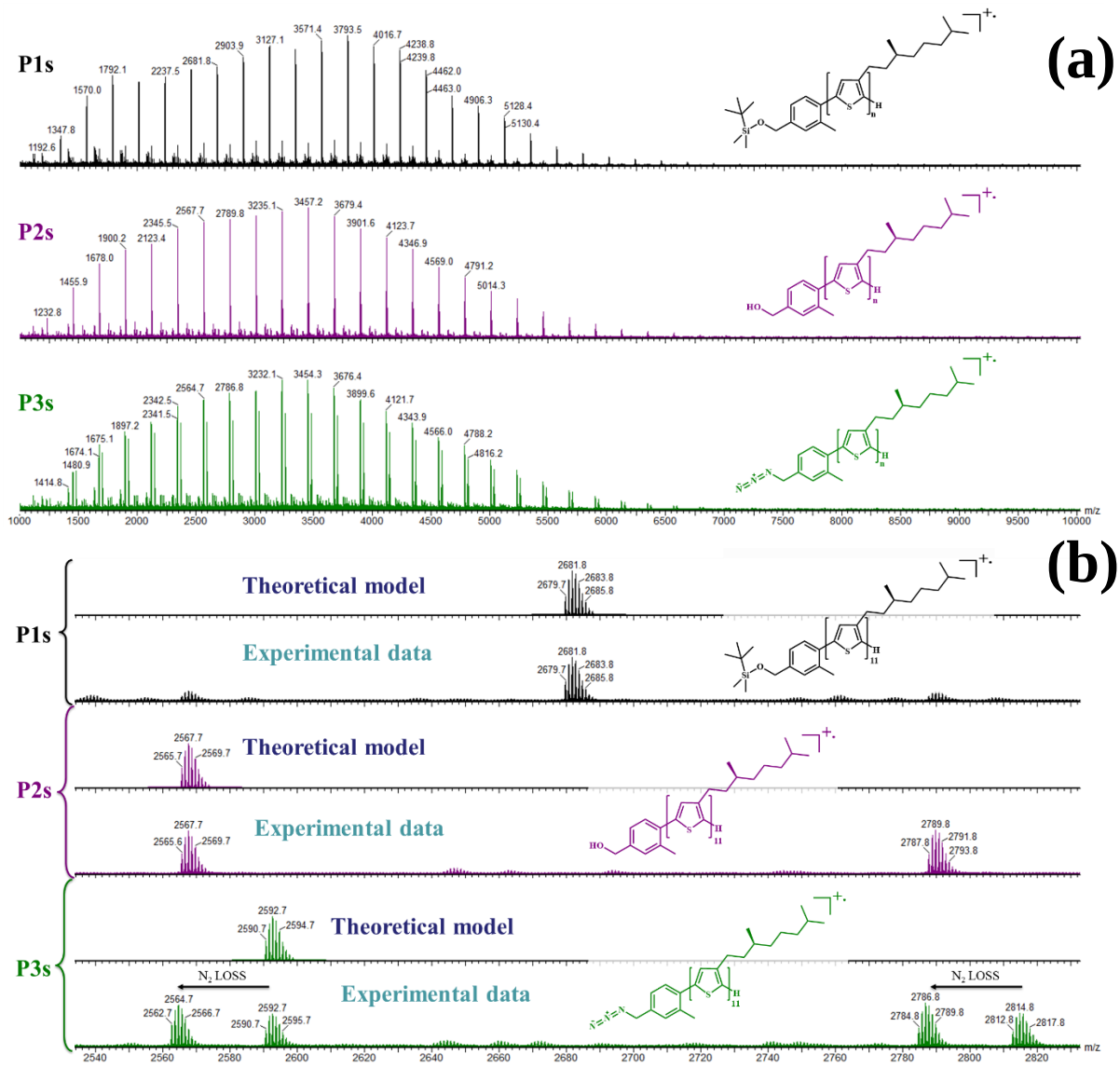

Figure S11. (a) global MALDI-ToF mass spectra for **P1a**-**P3a** and (b) magnification between *m/z* 2500 and m/z 2850 and comparison with isotopic model for 11-mers. Those mass spectra highlights the end-groups modification and proves the absence of degradation.

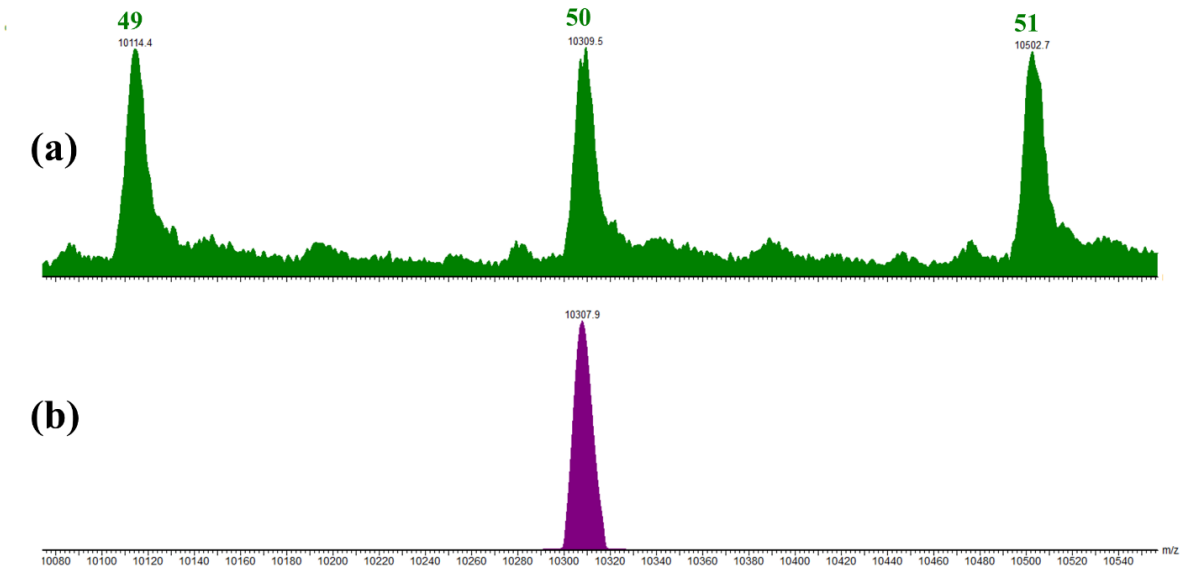

Figure S12. Comparison between experimental mass spectrum (a) for **P4a** and the theoretical isotopic model for the 50-mers star shaped polymer (b). The small difference in mass is due to the fact that is not the same isotope that is the most intense, it is explained by a contribution of the noise.

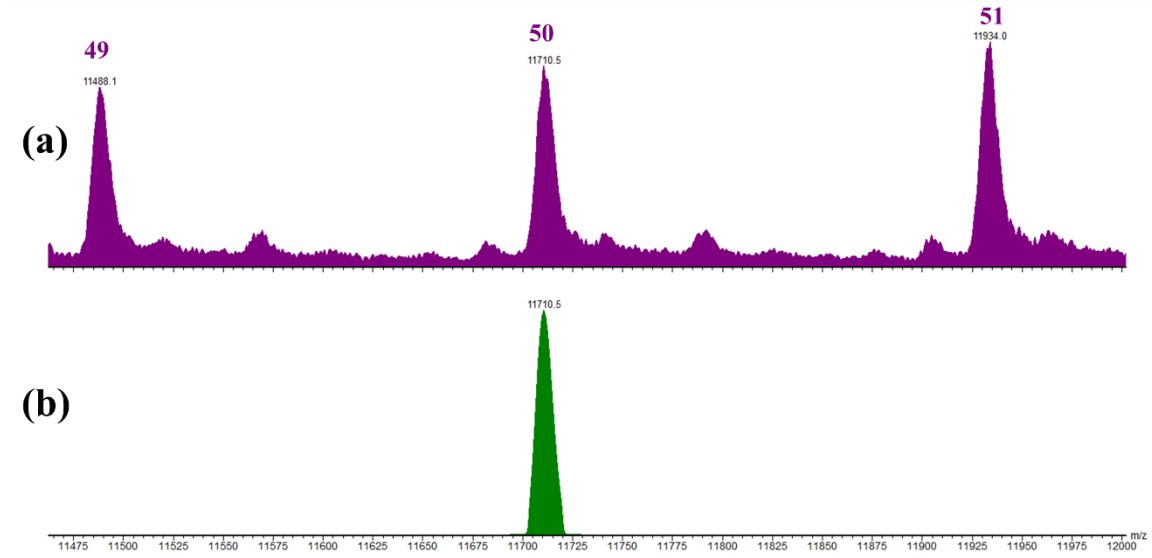

Figure S13. Comparison between experimental mass spectrum (a) for **P4s** and the theoretical isotopic model for the 50-mers star shaped polymer (b).

UV-VIS SPECTRA OF THE POLYMERS

The polymers are solubilized in chloroform ($CHCl_3$). Upon addition of methanol (MeOH) the polymers start to stack.

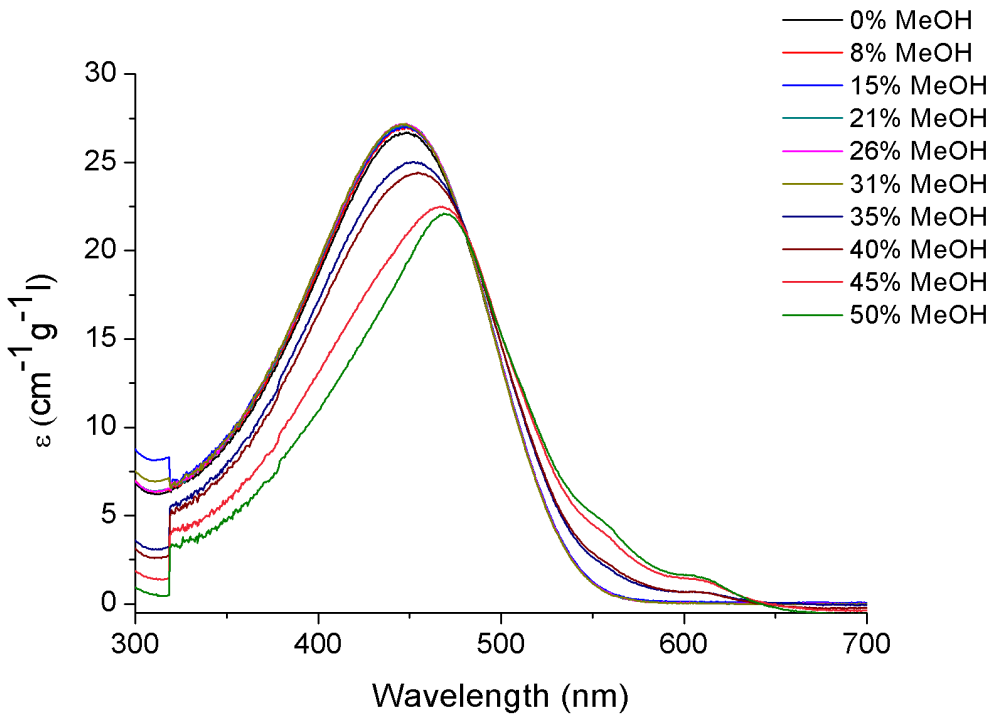

Figure S14. UV-vis spectra of **P3a** in $CHCl_3$ upon addition of methanol (MeOH).

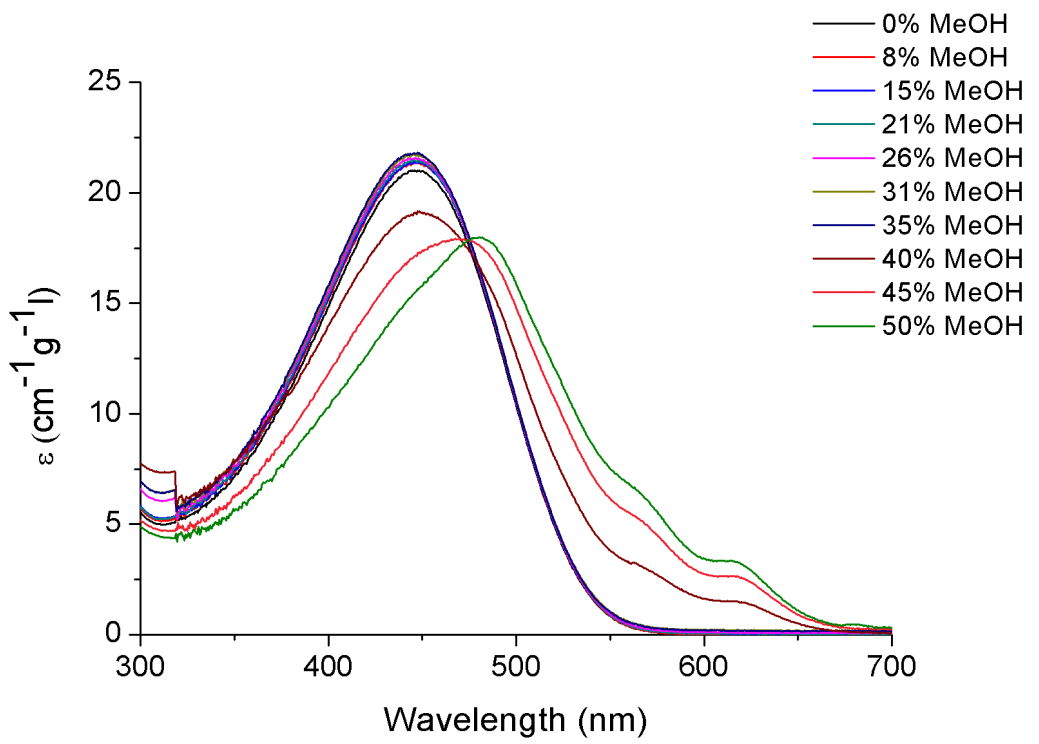

Figure S15. UV-vis spectra of **P3s** in $CHCl_3$ upon addition of methanol (MeOH).

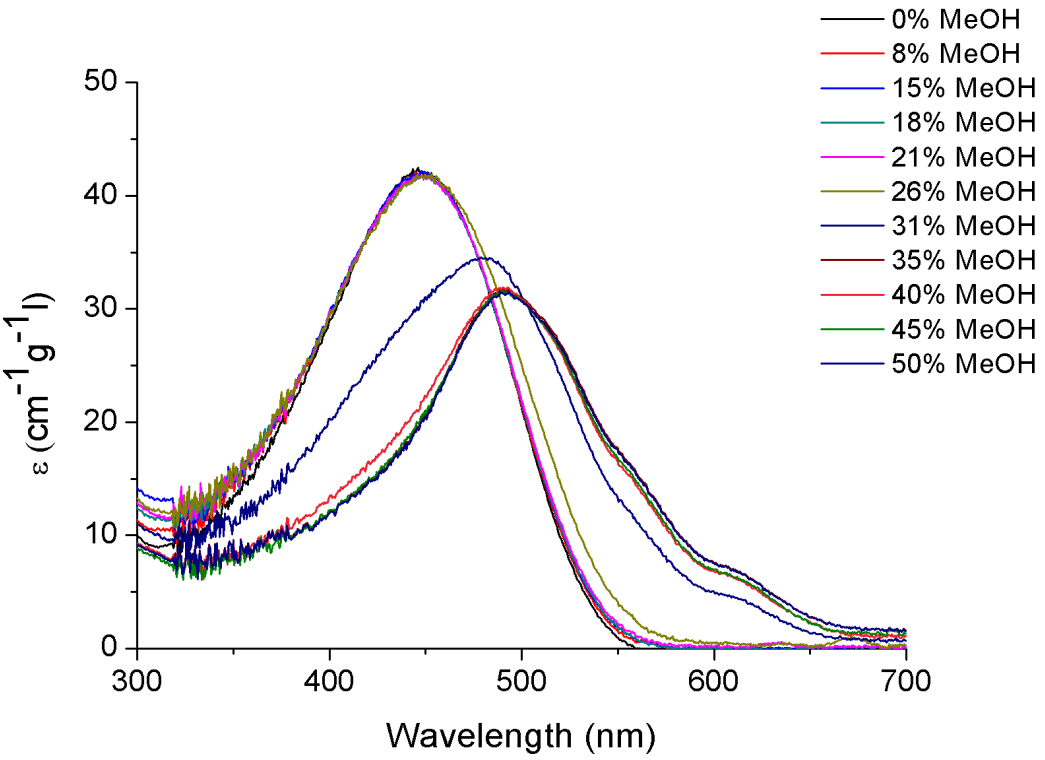

Figure S16. UV-vis spectra of **P4a** in $CHCl_3$ upon addition of methanol (MeOH).

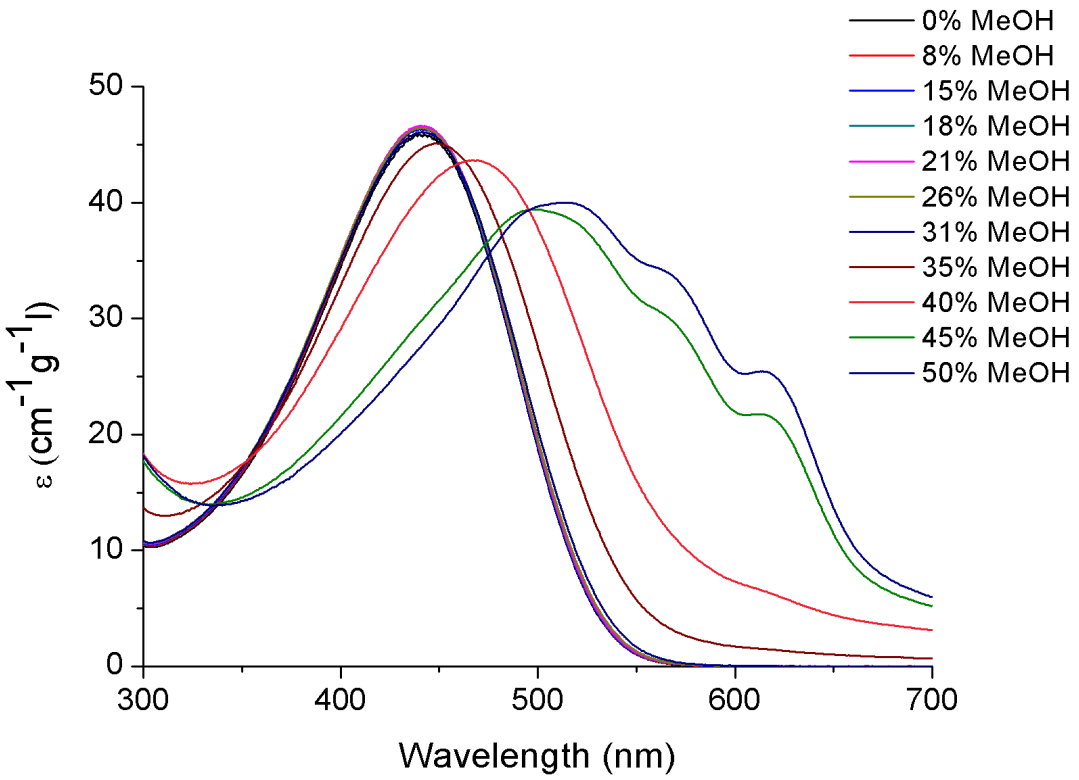

Figure S17. UV-vis spectra of **P4s** in $CHCl_3$ upon addition of methanol (MeOH).

CD-SPECTRA OF THE POLYMERS

The polymers are solubilized in chloroform ($CHCl_3$). Upon addition of methanol (MeOH) the polymers start to stack.

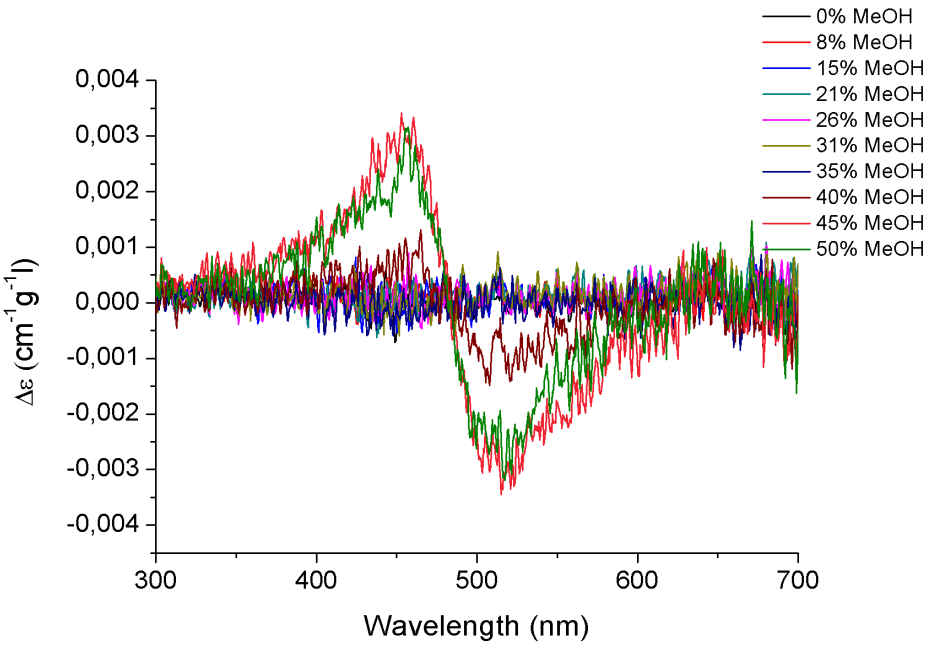

Figure S18. CD spectra of **P3s** in $CHCl_3$ upon addition of methanol (MeOH).

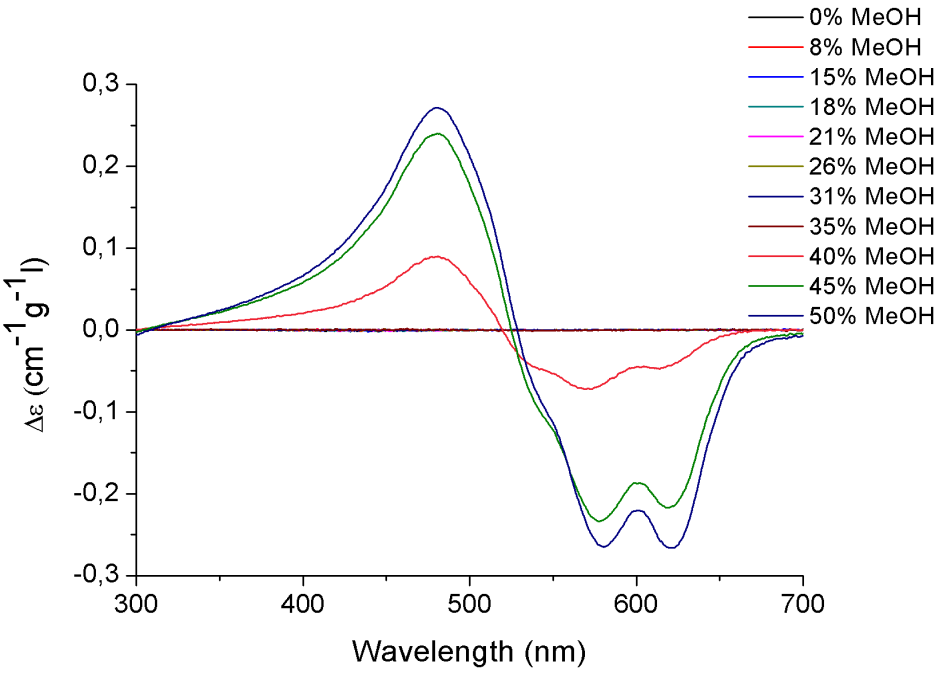

Figure S19. CD spectra of **P4s** in $CHCl_3$ upon addition of methanol (MeOH).

FLUORESCENCE SPECTRA OF THE POLYMERS

The obtained spectra have been divided by the absorbance obtained at the wavelength at which the polymers were excited. The wavelength of excitation is 400 nm and the spectra were recorded from 410 nm to 800 nm. For each sample 3 x 10 scans were taken. With these results the mean values and standard deviations have been calculated and plotted.

Fluorescence spectra of P3a

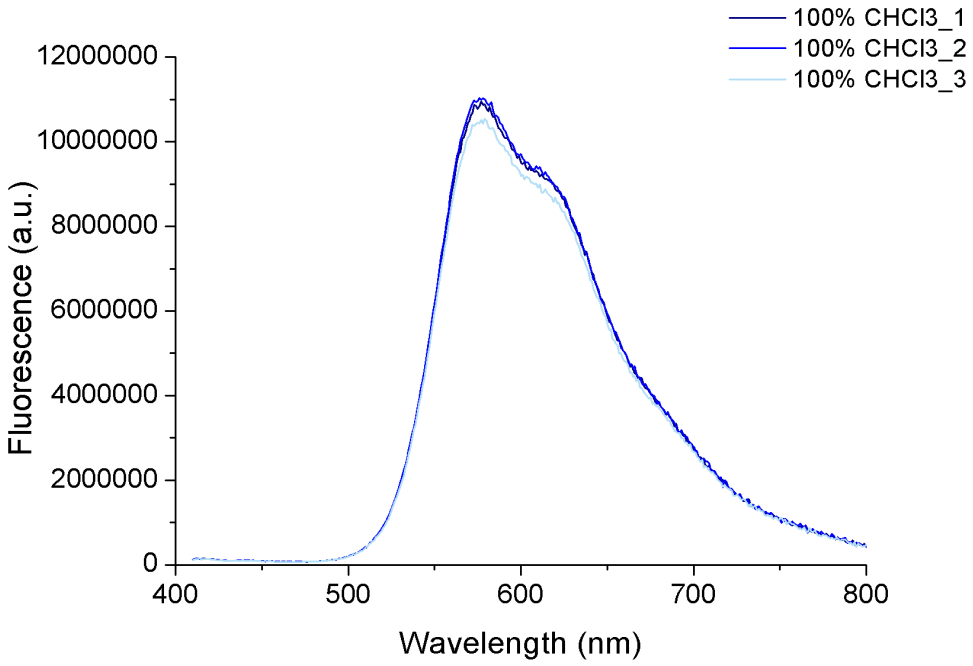

Figure S20. Fluorescence spectra of **P3a** in 100% $CHCl_3$.

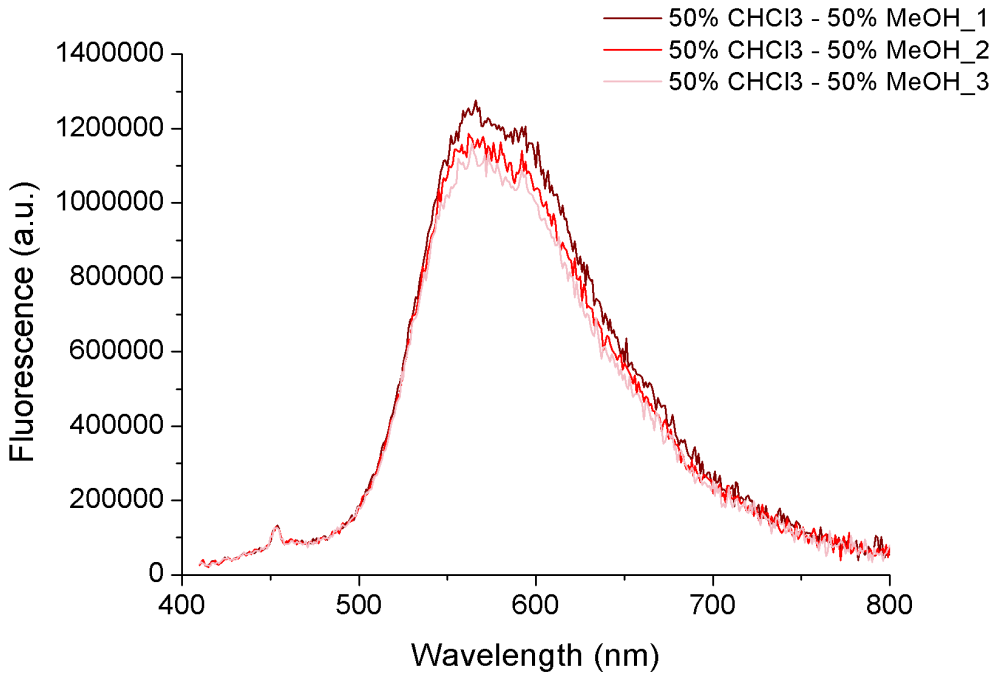

Figure S21. Fluorescence spectra of **P3a** in $CHCl_3$/MeOH (50/50).

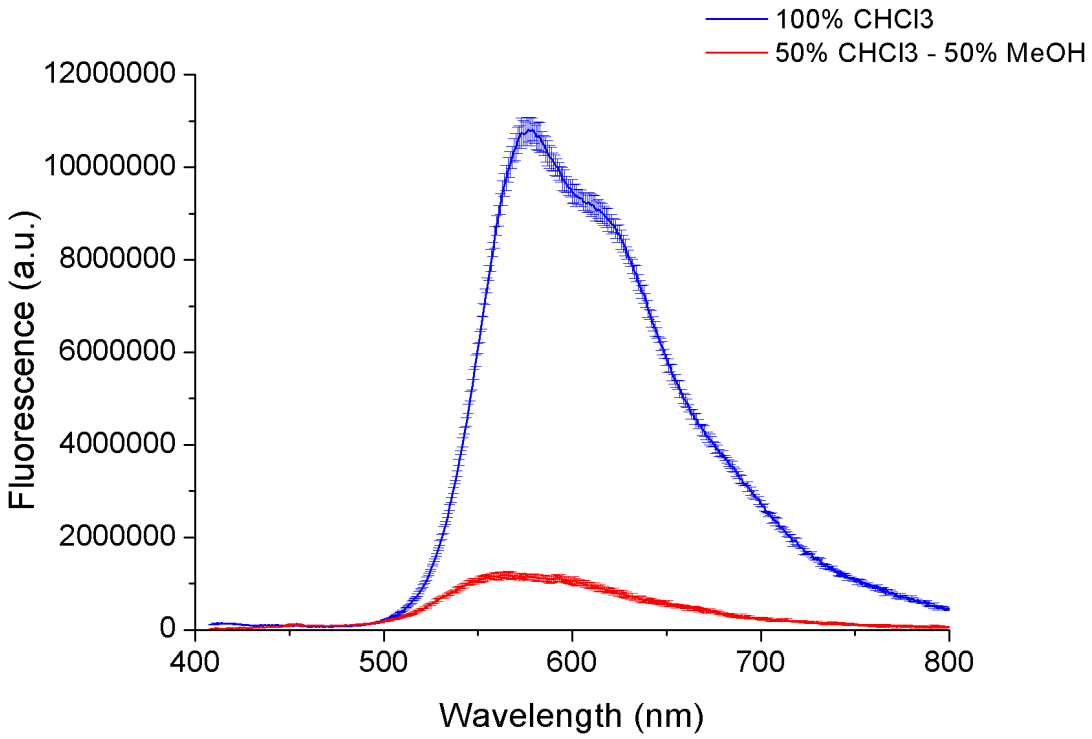

Figure S22. Fluorescence spectra of **P3a** in 100% $CHCl_3$ (blue) and $CHCl_3$/MeOH (50/50) (red). The mean value is given together with the standard deviation.

Fluorescence spectra of P3s

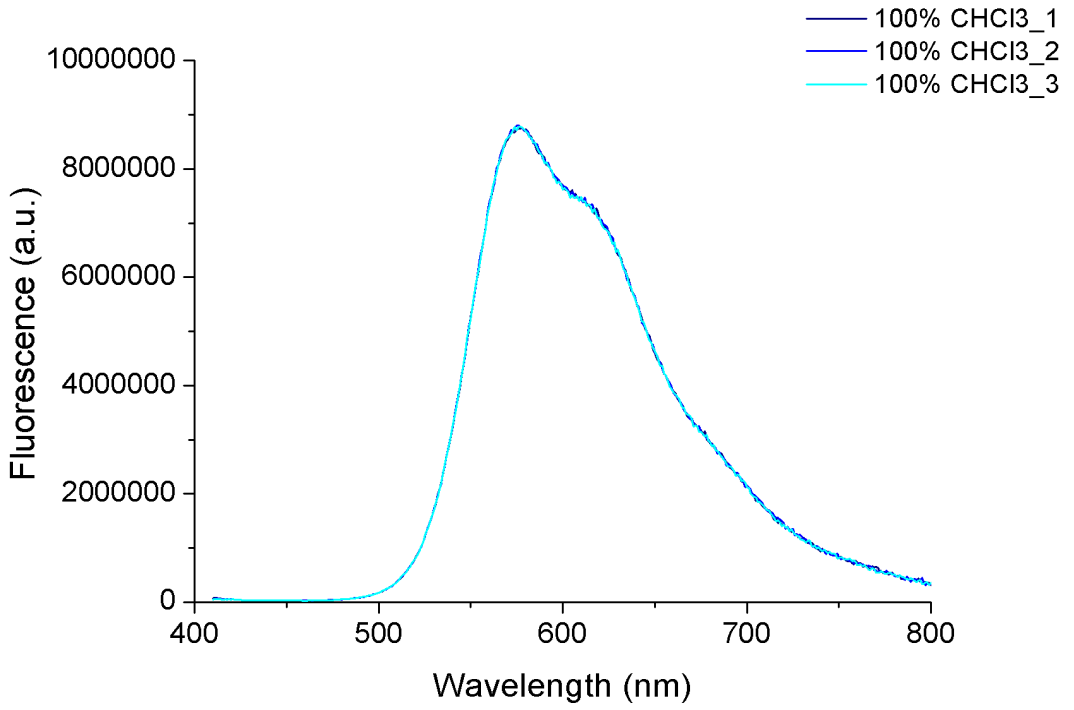

Figure S23. Fluorescence spectra of **P3s** in 100% $CHCl_3$.

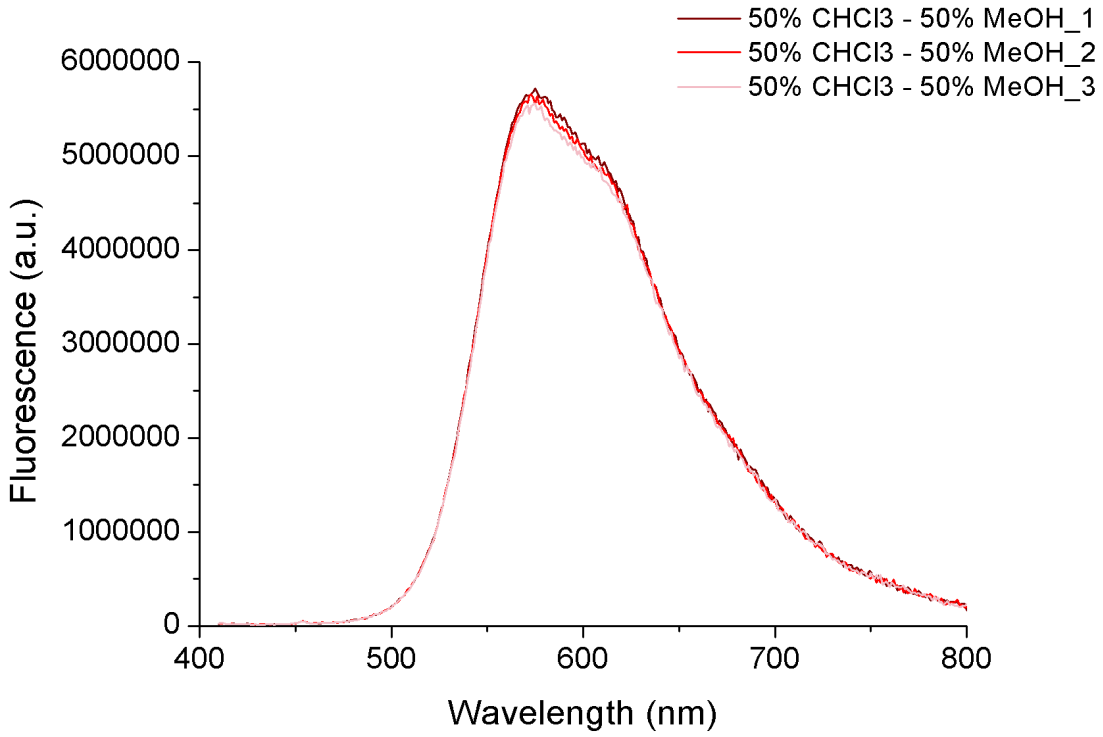

Figure S24. Fluorescence spectra of **P3s** in $CHCl_3$/MeOH (50/50).

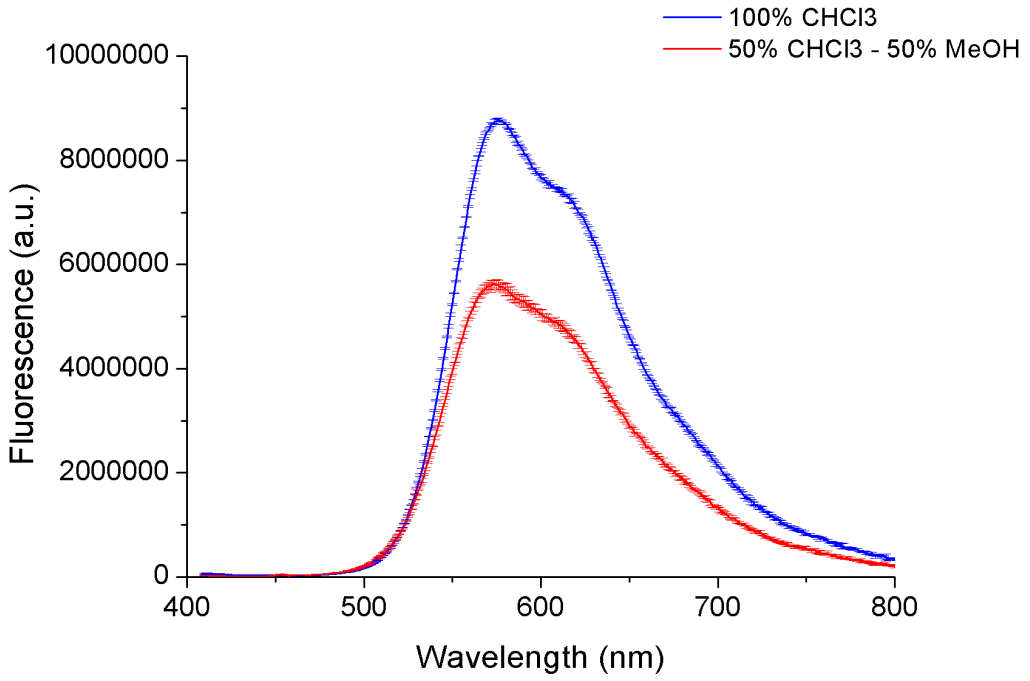

Figure S25. Fluorescence spectra of **P3s** in 100% $CHCl_3$ (blue) and $CHCl_3$/MeOH (50/50) (red). The mean value is given together with the standard deviation.

Fluorescence spectra of P4a

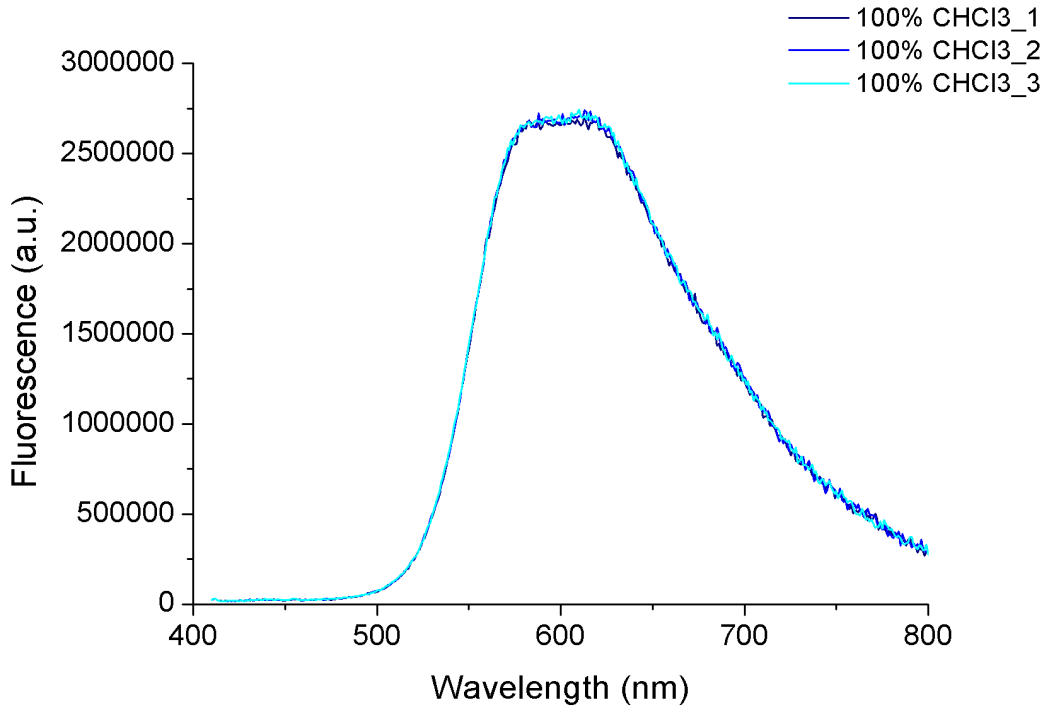

Figure S26. Fluorescence spectra of **P4a** in 100% $CHCl_3$.

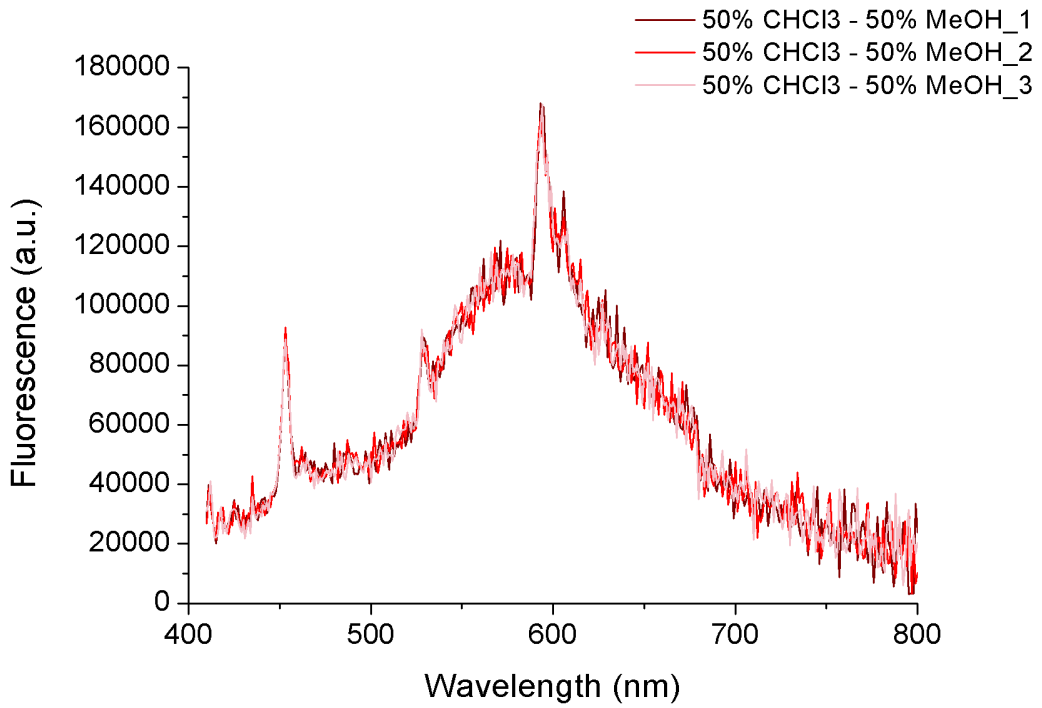

Figure S27. Fluorescence spectra of **P4a** in $CHCl_3$/MeOH (50/50).

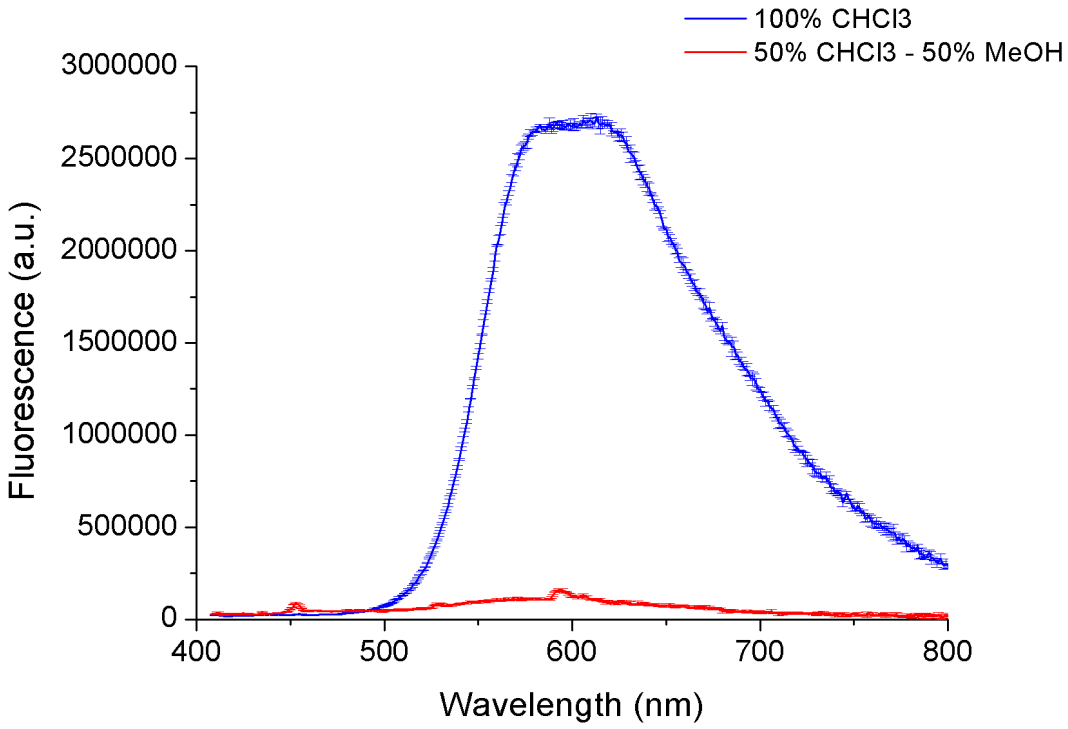

Figure S28. Fluorescence spectra of **P4a** in 100% $CHCl_3$ (blue) and $CHCl_3$/MeOH (50/50) (red). The mean value is given together with the standard deviation.

Fluorescence spectra of P4s

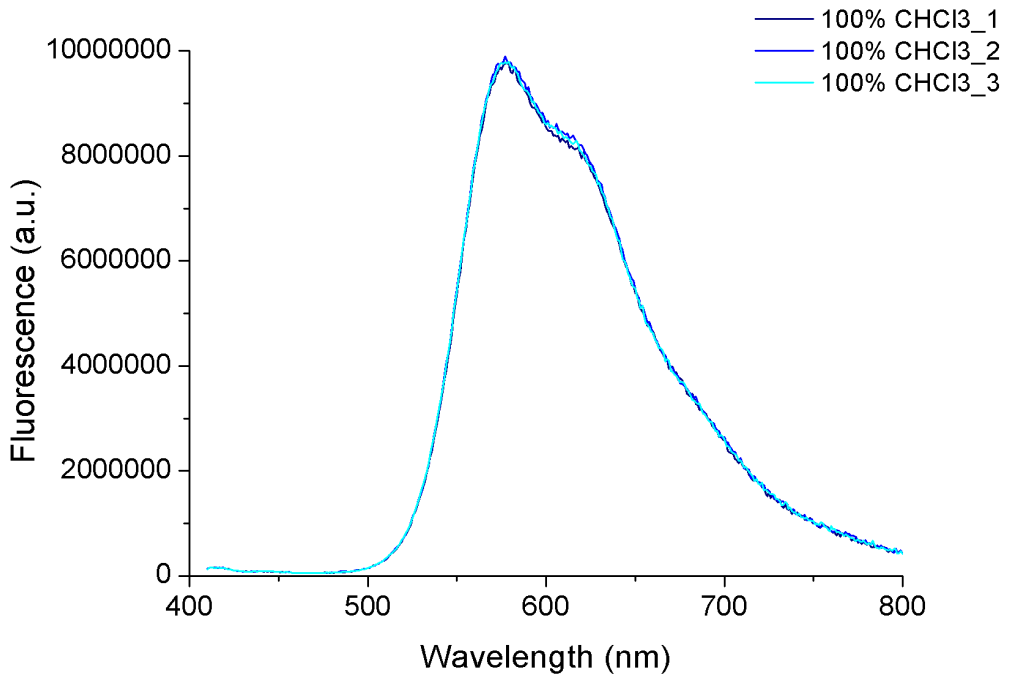

Figure S29. Fluorescence spectra of **P4s** in 100% $CHCl_3$.

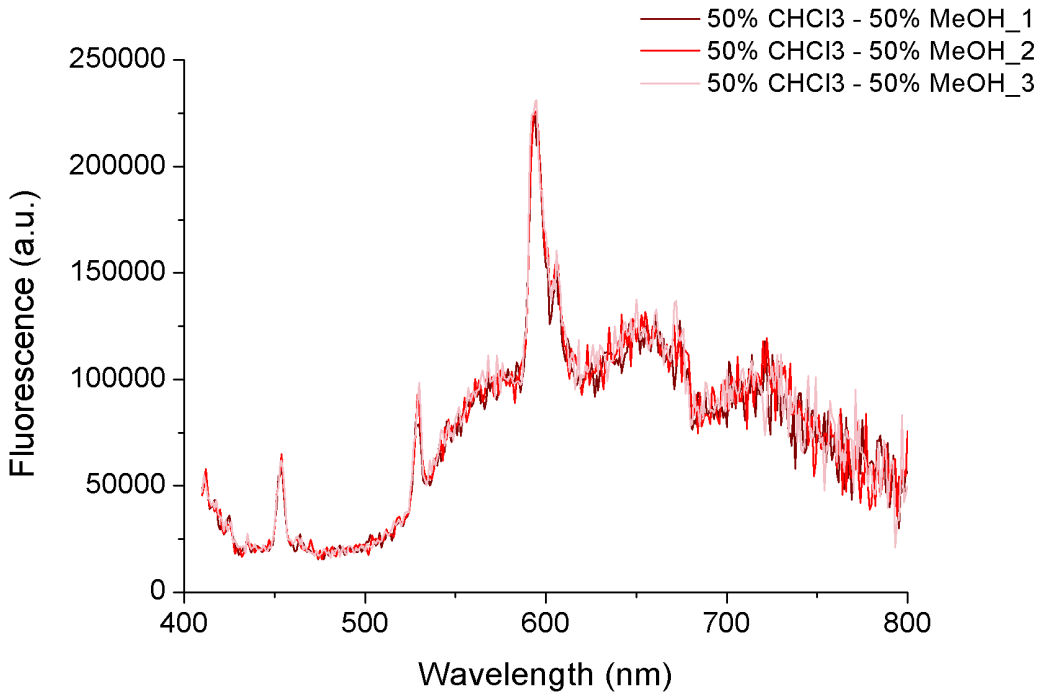

Figure S30. Fluorescence spectra of **P4s** in $CHCl_3$/MeOH (50/50).

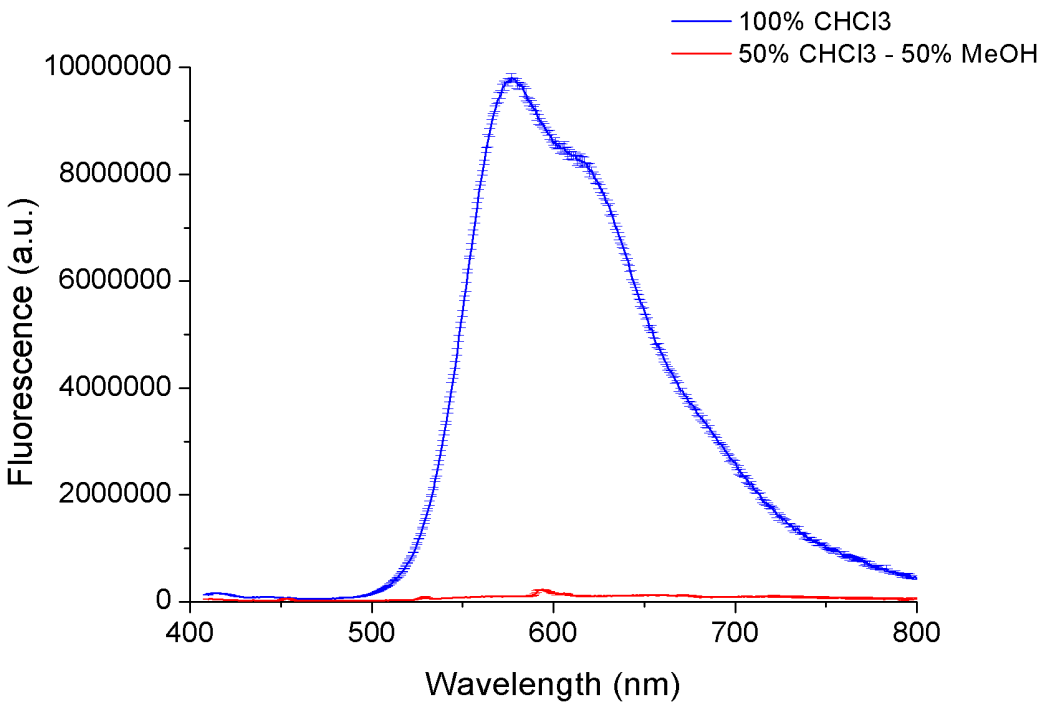

Figure S31. Fluorescence spectra of **P4s** in 100% $CHCl_3$ (blue) and $CHCl_3$/MeOH (50/50) (red). The mean value is given together with the standard deviation.

DSC SPECTRA OF THE POLYMERS

DSC of P3s

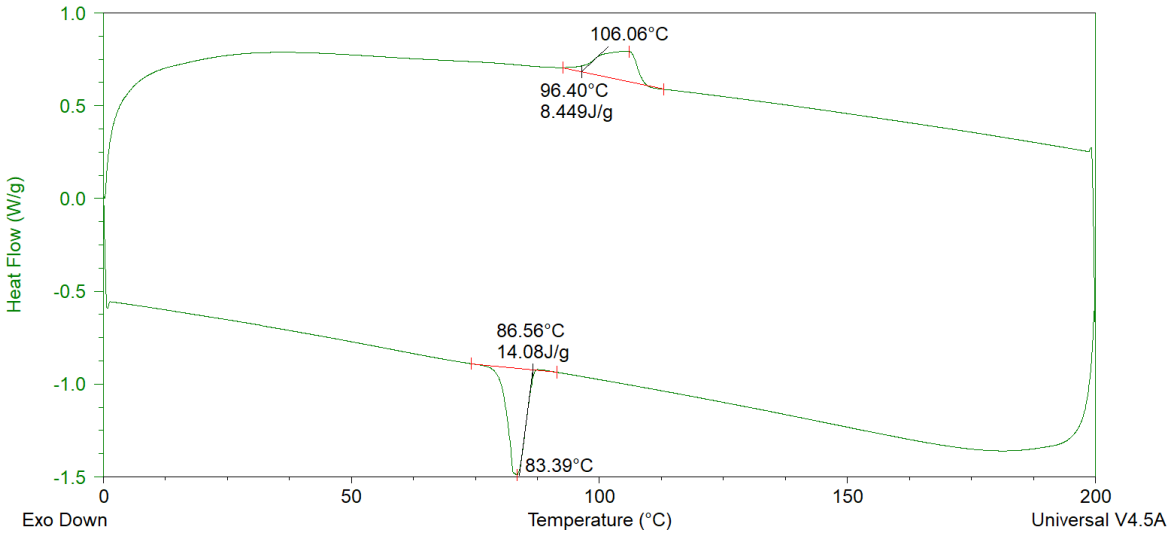

Figure S32. DSC of **P3s**.

DSC of P3a

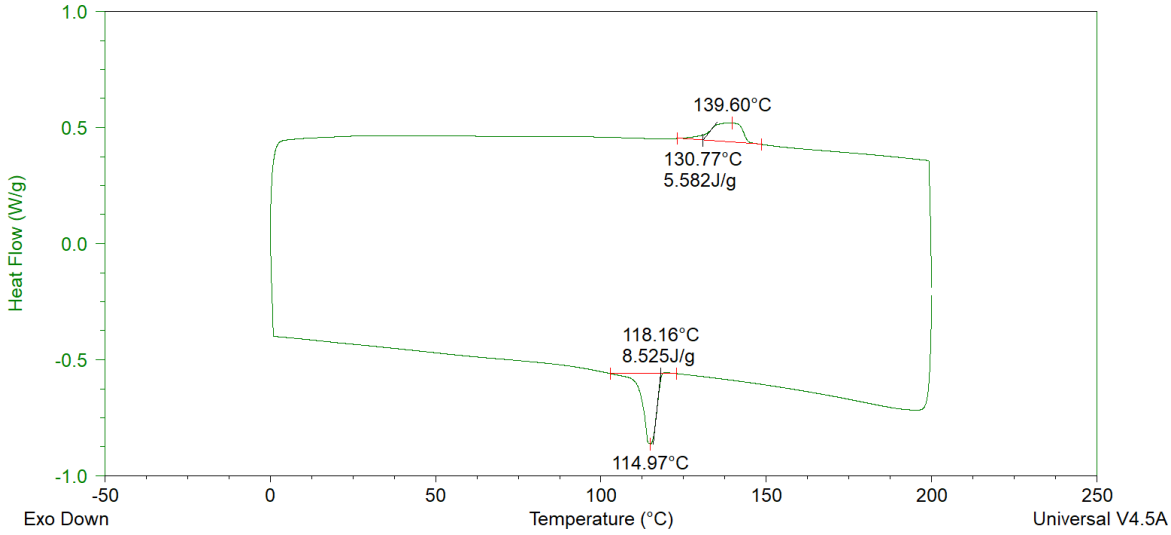

Figure S33. DSC of **P3a**

DSC of P4s

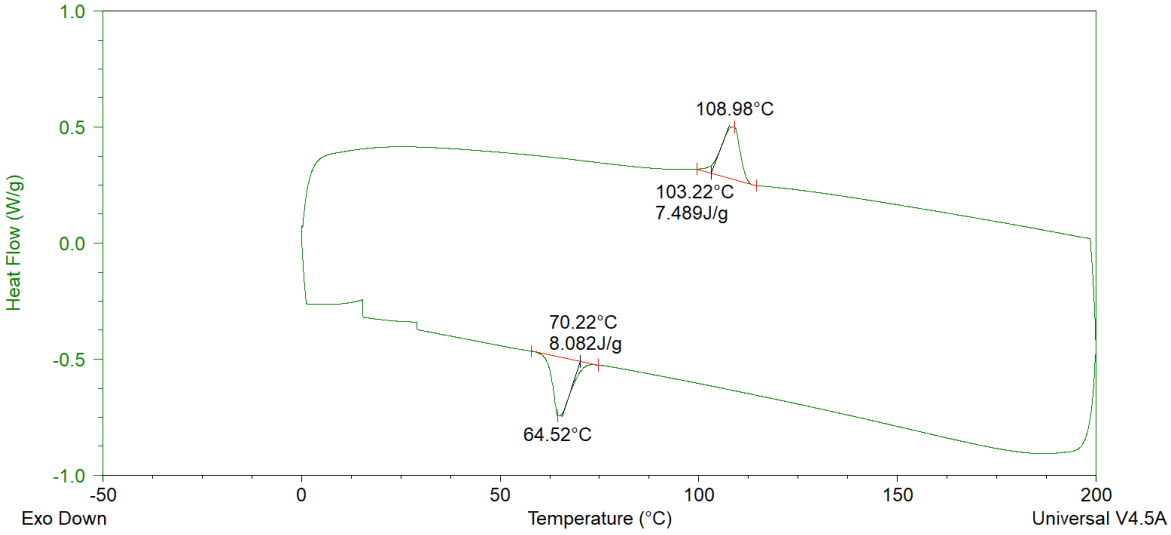

Figure S34. DSC of **P4s**.

DSC of P4a

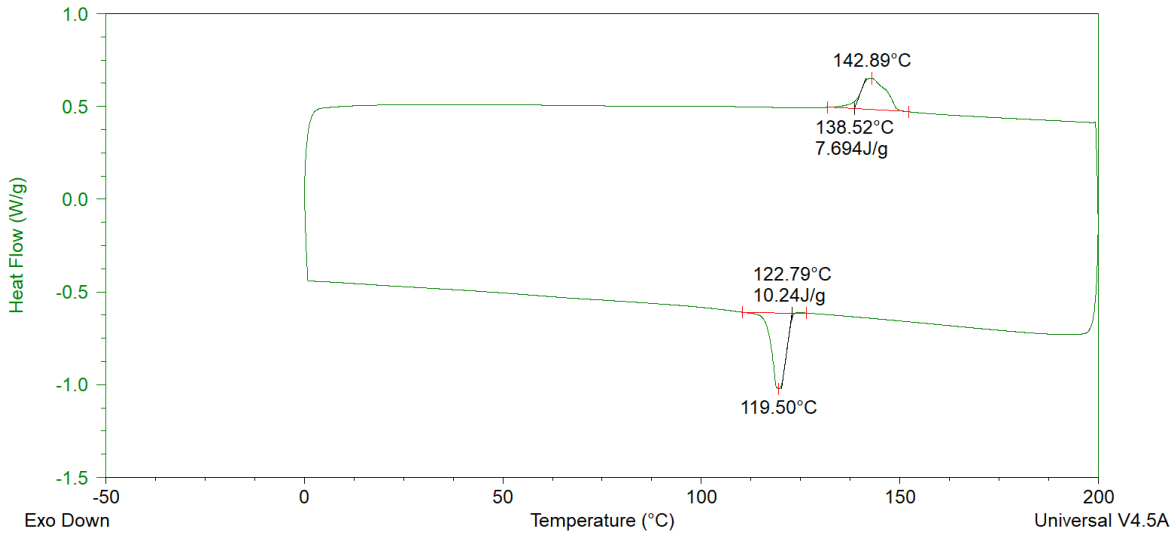

Figure S35. DSC of **P4a**.

AFM MEASUREMENTS OF THE POLYMERS

Dry films for AFM analysis were all prepared using the same drop-casting protocol for the four different polymers. Solutions of the same concentrations (0.1 mg/ml) were deposited from varying solvents (chloroform, toluene, and chloroform/methanol mixture) to find for each polymer the solvent that favors the most the formation of neat self-assembled structures. In every case the polymers were present on the surface as inhomogeneous films, with regions being either empty, partially covered, covered by a uniform poly(thiophene) monolayer or covered by multilayer aggregates.

Samples of **P3a** on graphite prepared from chloroform and chloroform/methanol solutions exhibited some regions with films of uniform thickness (≈ 1.5 nm) typical of a monolayer (Figures S36-37). This observation suggests that all the polymers were standing edge-on, and probably stabilized by π-stacking, but no internal lamellar organization could be observed. As a consequence, those films showed no long-range ordered (or poorly ordered) supramolecular structures, and did not allow studying the self-assembly behavior of the polymer.

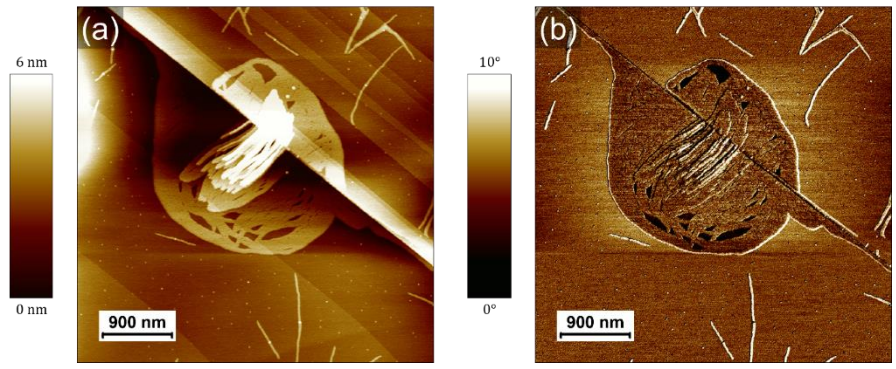

Figure S36. AFM topography (a) and phase (b) large scale images of a dry film of **P3a**, prepared by drop-casting a 0.1 mg/ml solution in chloroform on graphite. The polythiophenes form a patch with varying height, the bottom layer having a thickness (≈ 1.5 nm) compatible with a monolayer. No order is observed within the film.

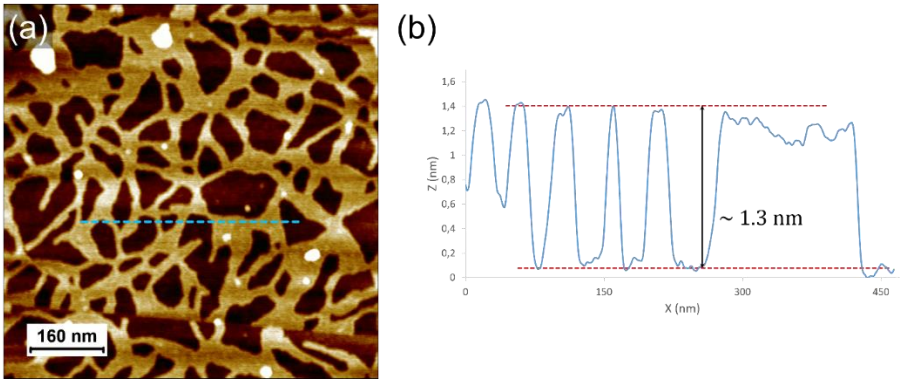

Figure S37. (a) AFM topography image of a dry film of **P3a**, prepared by drop-casting a 0.1 $mg.ml^{-1}$ solution in a chloroform/methanol mixture on graphite (a 0.2 mg/ml solution in chloroform was first drop-casted and then an equal volume of methanol was added on surface). No order is observed within the film. (b) Line profile along the blue dotted line in panel (a) shows a homogeneous thickness compatible with a monolayer of polythiophenes.

As opposed, samples of **P3a** prepared from toluene solutions exhibited highly ordered lamellar structures, as shown in the main text and in Figure S38. In these structures, observed either in mono- or bi-layers, the fibers (formed themselves by polythiophenes self-assembled through

π-stacking) are juxtaposed together in an ordered fashion to give rise to self-assembled superstructures.

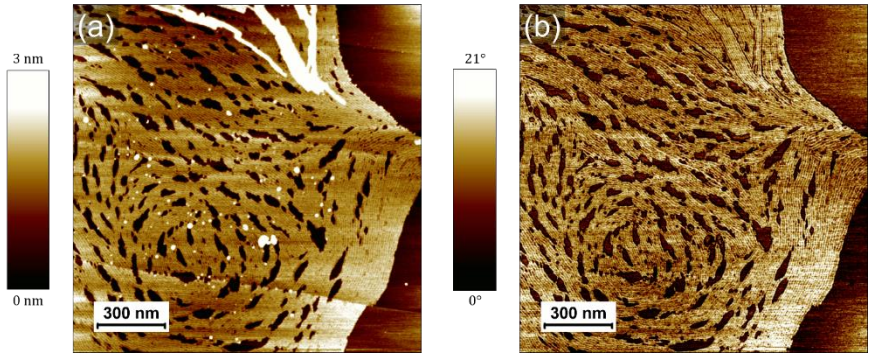

Figure S38. AFM topography (a) and phase (b) large scale images of a dry film of **P3a**, prepared by drop-casting a 0.1 mg/ml solution in toluene on graphite. Most of the region is covered by a monolayer organized in lamellar fashion. A second layer also organized into lamellae can also be seen in the brighter region on the top of the topography image.

Samples of **P4a** showed fibers formation from both chloroform and toluene solutions. In the case of chloroform, fibers were present as: isolated fibers in sub-monolayer regions, long-range ordered lamellae in bilayer regions and poorly ordered multilayer aggregates.

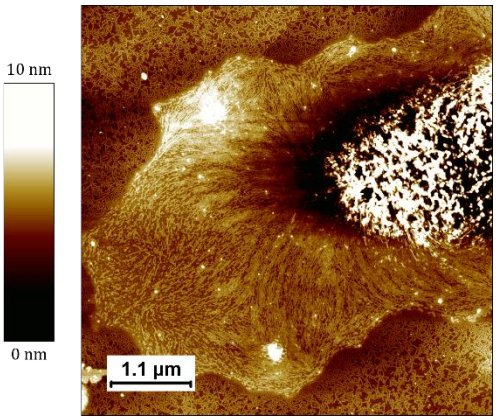

Figure S39. Large scale AFM topography image of a dry film of **P4a**, prepared by drop-casting a 0.1 mg/ml solution in chloroform on graphite showing the coexistence of several regions: sub-monolayer coverage by individual fibers (lower part), second layer exhibiting

lamellar order (center of the image) and multilayer patch (brighter region). A high resolution image taken in the second-layer region is shown in Figure 7b of the main text.

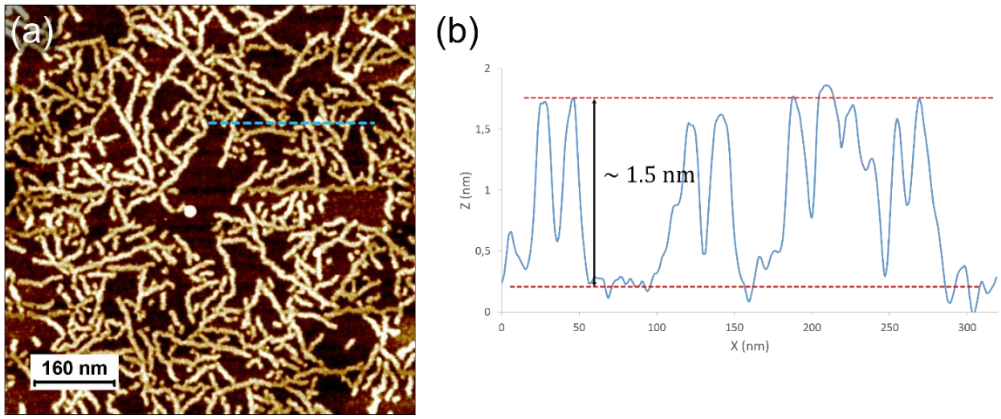

Figure S40. (a) AFM topography image of a dry film of **P4a**, prepared by drop-casting a 0.1 mg/ml solution in chloroform on graphite, and showing individual fibers covering partially the surface. (b) Line profile along the blue dotted line in panel (a) shows a fibers thickness compatible with a monolayer of polythiophenes.

Samples of **P4a** prepared from toluene exhibited regions with uniform monolayers composed of regularly ordered fibers.

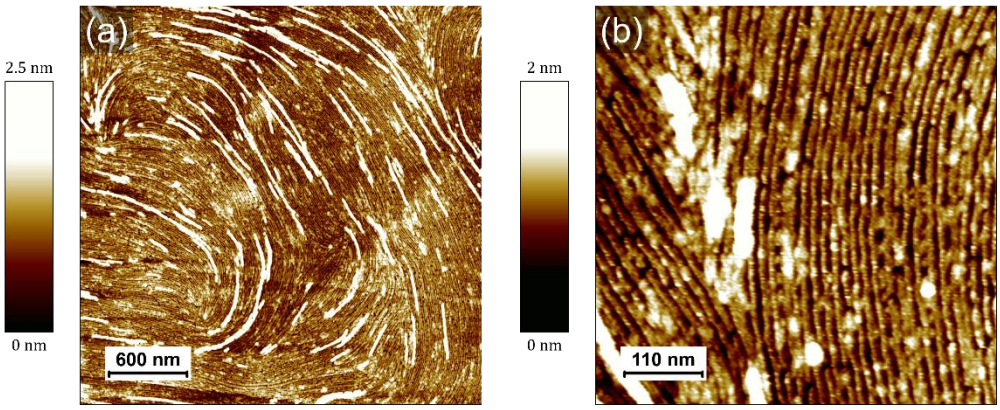

Figure S41. Large scale (a) and high resolution (b) AFM topography images of a dry film of **P4a**, prepared by drop-casting a 0.1 mg/ml solution in toluene on graphite. The bottom layer

is composed of densely packed fibers regularly ordered in a lamellar superstructure. The brighter zones correspond to a second layer of polythiophene fibers on top of the first one.

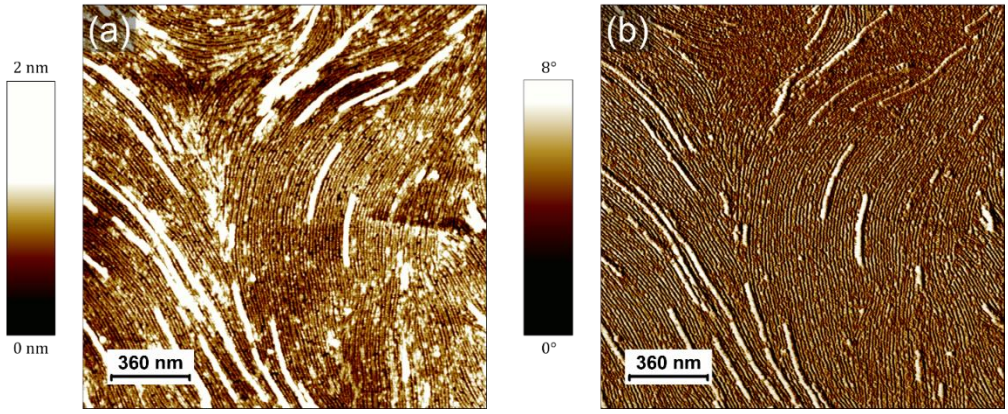

Figure S42. AFM topography (a) and phase (b) images of a dry film of **P4a**, prepared by drop-casting a 0.1 mg/ml solution in toluene on graphite.

For samples of **P3s**, only samples prepared from toluene solutions could show some fibrous structures (main text). No organization was observed at all after drop-casting from chloroform and chloroform/methanol mixture.

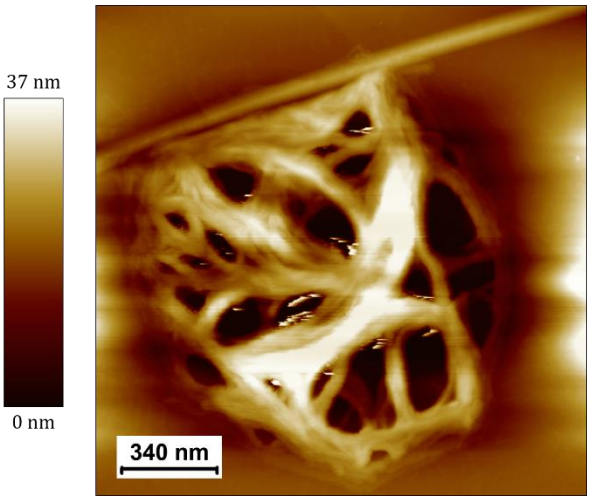

Figure S43. AFM topography image of a dry film of **P3s**, prepared by drop-casting a 0.1 mg/ml solution in toluene on graphite. Intertwined fibers tend to aggregate to form thick patches on the surface.

For samples of **P4s**, only samples prepared from chloroform solutions could show fibers, present only in thick aggregates (main text). No organization was observed at all after drop-casting from toluene and chloroform/methanol mixture.

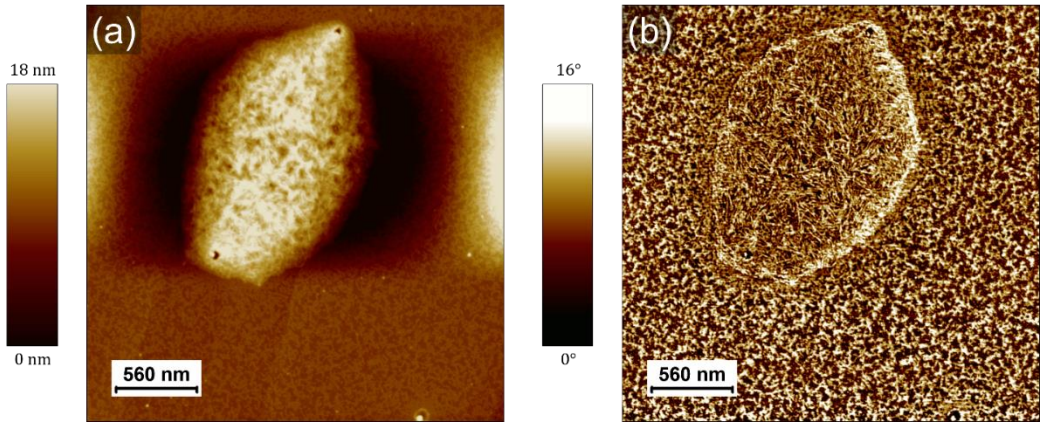

Figure S44. AFM topography (a) and phase (b) images of a dry film of **P4s**, prepared by drop-casting a 0.1 mg/ml solution in chloroform on graphite. The thick aggregate on the top part of the image is composed of fibers (a higher resolution image in shown in the Figure 7 of the main text). The rest of the surface is partially covered with a monolayer-thick film showing no apparent internal order (similar to what is shown in the image of **P4a** in Figure S44).

THEORETICAL CALCULATION FOR WIDTH OF FIBER

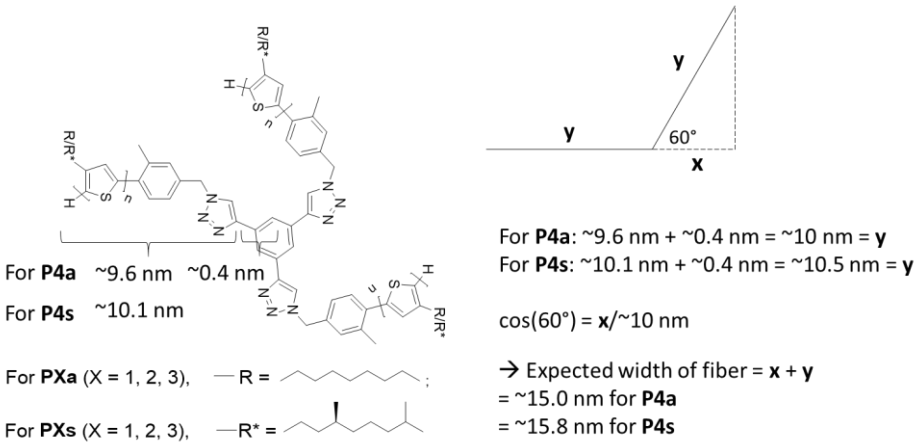

Figure S45. Theoretical calculation of the width of the fiber expected for **P4a** and **P4s**.

TEM MEASUREMENT

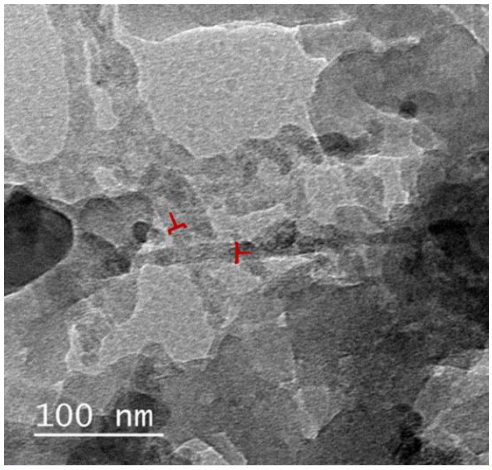

Figure S46. TEM measurement of **P4s**.

GPC SPECTRA OF THE POLYMERS

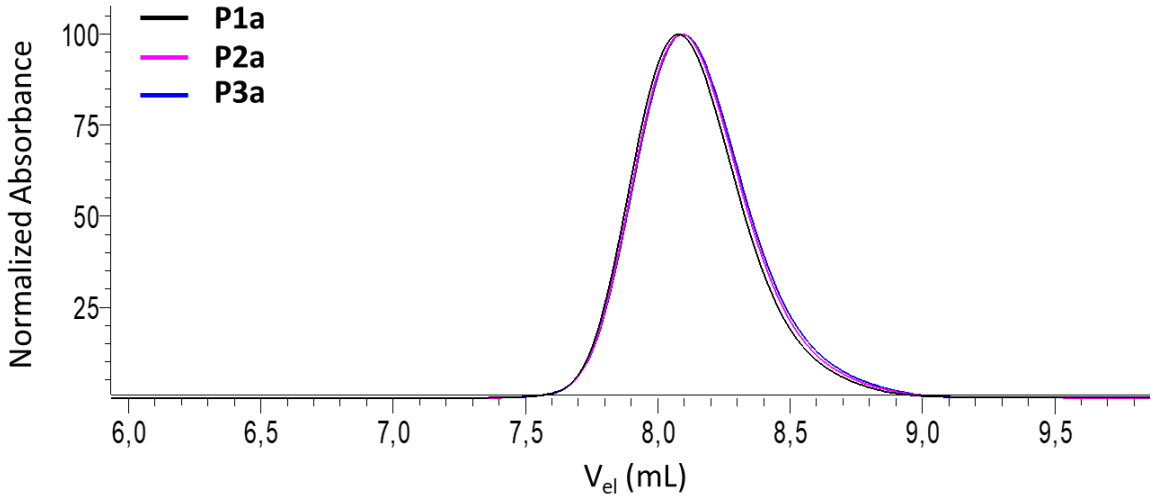

Figure S47. GPC measurements of polymers **P1a**, **P2a** and **P3a**.

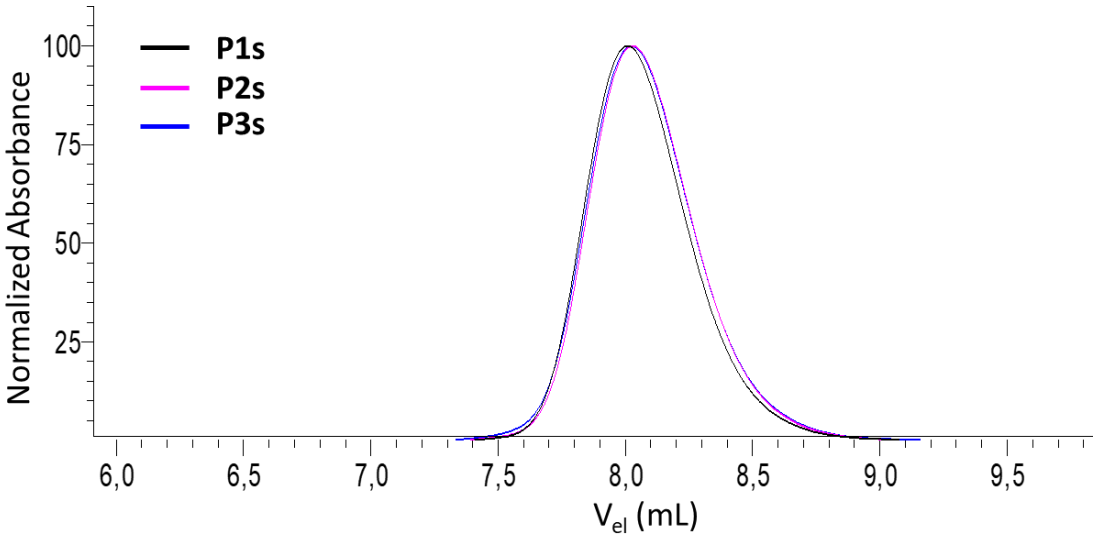

Figure S48. GPC measurements of polymers **P1s**, **P2s** and **P3s**.

REFERENCES

(1) Verswyvel, M.; Monnaie, F.; Koeckelberghs, G. AB Block copoly(3-Alkylthiophenes): Synthesis and Chiroptical Behavior. *Macromolecules* **2011**, *44* (24), 9489–9498.

(2) Smeets, A.; Van Den Bergh, K.; De Winter, J.; Gerbaux, P.; Verbiest, T.; Koeckelberghs, G. Incorporation of Different End Groups in Conjugated Polymers Using Functional Nickel Initiators. *Macromolecules* **2009**, *42* (20), 7638–7641.

(3) Horcas, I.; Fernández, R.; Gómez-Rodríguez, J. M.; Colchero, J.; Gómez-Herrero, J.; Baro, A. M. WSXM: A Software for Scanning Probe Microscopy and a Tool for Nanotechnology. *Review of Scientific Instruments* **2007**, *78* (1).